# Electron scattering from vector- and tensor-polarized deuteron
## Introduction and Legacy of NIKHEF and MIT-Bates

S. Širca, U of Ljubljana, Slovenia

EIC Light Ion Study Group, May 27, 2026


Montauk Point Lighthouse (1796) before 1899

# Deuteron's first ≈ 100 years

## Proposed in 1931

The chemical value[7] is $1.00777 \pm 0.00002$ (probable error), as compared with Aston's $1.00778 \pm 0.00015$ (*limit* of error). Aston's value, reduced to the chemical scale, is 1.00756 and the discrepancy appears to be outside the limits of error. It could be removed by postulating the existence of an isotope of hydrogen of mass 2, with a relative abundance $H^1/H^2 = 4500$. It should be possible, although difficult, to detect such an isotope by means of band spectra.

Birge, Menzel, PR **37**, 1669 (1931)

## Discovered in 1932

They are not molecular lines for they do not appear on a plate taken with the discharge tube in the "white stage" with the molecular spectrum enhanced ($H^2_\gamma$ was found as a slight irregularity on a microphotometer curve of this plate). Finally the $H^2_\alpha$ line is resolved into a doublet with a separation of about 0.16A in agreement with the observed separation of the $H^1_\alpha$ line.

The relative abundance in ordinary hydrogen, judging from relative minimum exposure time is about 1:4000, or less, in agreement with Birge and Menzel's estimate. A similar estimate of the abundance in the second sample indicated a concentration of about 1 in 800. Thus an appreciable fractionation has been secured as expected from theory.[4]

Urey, Brickwedde, Murphy, PR **39**, 164 (1932), $1\frac{1}{2}$ p!
(actual abundance 1 : 6420 = 156 ppm)

- Urey: Nobel Prize in Chemistry 1934
- Chadwick: neutron 1932, Nobel Prize in Physics 1935

# Deuteron as a nonrelativistic 2N bound state



General form of the NN-potential for $T = 0$, $S = 1$:

$$V(T=0,S=1) = V_{01}^{\rm c}(r) + V_{01}^{\rm t}(r) S_{12} + V_{01}^{\rm ls}(r) \boldsymbol{L}\cdot\boldsymbol{S} + V_{01}^{\rm l2}(r) \boldsymbol{L}^2 + V_{01}^{\rm ls2}(r) (\boldsymbol{L}\cdot\boldsymbol{S})^2$$

central tensor spin-orbit orbital quad. spin-orbit

$$S_{12} \propto 3(\hat{\boldsymbol{r}}\cdot\boldsymbol{\sigma}_1)(\hat{\boldsymbol{r}}\cdot\boldsymbol{\sigma}_2) - \boldsymbol{\sigma}_1\cdot\boldsymbol{\sigma}_2$$

$$\langle M_S = 0 | V_{01}^{\rm stat} | M_S = 0 \rangle = V_{01}^{\rm c}(r) - 4V_{01}^{\rm t}(r) P_2(\cos\theta)$$

$$\langle M_S = \pm 1 | V_{01}^{\rm stat} | M_S = \pm 1 \rangle = V_{01}^{\rm c}(r) + 2V_{01}^{\rm t}(r) P_2(\cos\theta)$$

$\theta$ = polar angle of $\boldsymbol{r}$ wrt. quantization axis

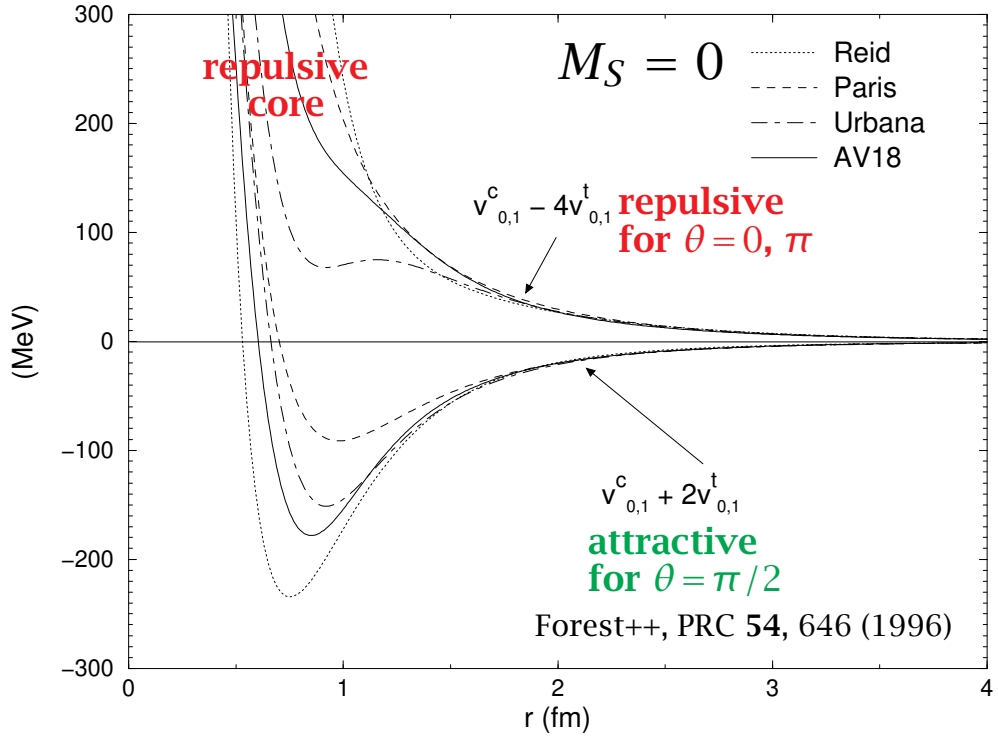

# Deuteron as a nonrelativistic 2N bound state



- At $r \gtrsim 1.5$ fm, $V_{01}^{\mathrm{stat}}$ dominated by one-pion exchange
- Significant model dependence at small $r$, but it is largely cancelled by differences in the momentum-dependent terms in the models

  Note: Modern NN potentials are all phase-shift equivalent. This does not mean that the models involving them are identical. See e.g. Polls++, PLB **432**, 1 (1998)
- $\langle 0|V_{01}^{\mathrm{stat}}|0\rangle$ has a repulsive core; outside attractive for $\theta = \pi/2$ and repulsive for $\theta = 0, \pi \implies$ np pairs form a **toroidal** density in $(x, y)$-plane
- $\langle \pm 1|V_{01}^{\mathrm{stat}}| \pm 1\rangle$ has two minima, separated by a barrier $\implies$ the np-pair density has a **dumbbell** shape

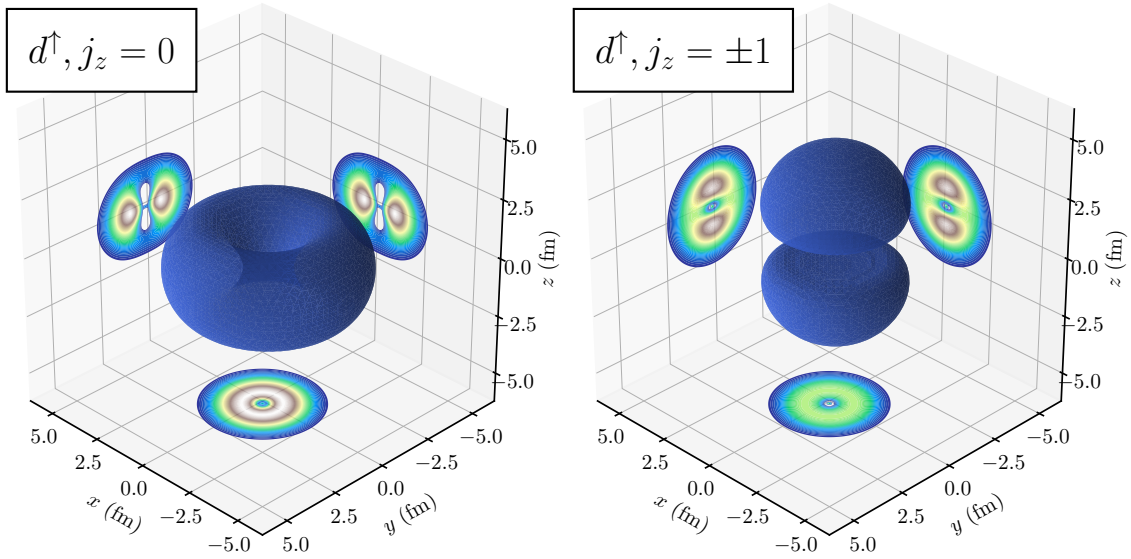


Mäntysaari++, PLB **858**, 139052 (2024)

To see how this comes about, consider the deuteron wave-function:

$$\psi^M_{LSJ}(\boldsymbol{r}) = R_0(r)\,\mathcal{Y}^M_{011}(\hat{\boldsymbol{r}}) + R_2(r)\,\mathcal{Y}^M_{211}(\hat{\boldsymbol{r}})$$

▷ Spin-angle wave-functions: $\mathcal{Y}^M_{LSJ}(\hat{\boldsymbol{r}}) = \sum_{M_L M_S} C^{JM}_{LM_L SM_S} Y_{LM}(\hat{\boldsymbol{r}})|SM_S\rangle$

▷ $S$- and $D$-state radial wave-functions: $R_0(r) \equiv u(r)/r$, $R_2(r) \equiv w(r)/r$

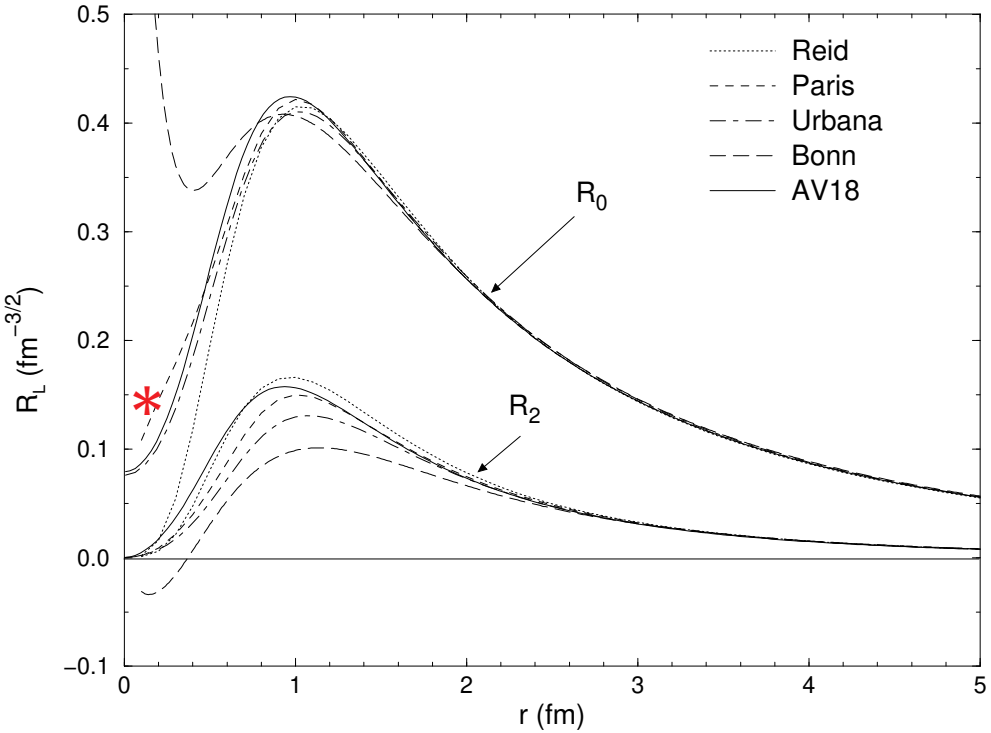


∗ $S$-wave WF reduced at small $r \Longrightarrow$ node in Four. transform at $p \approx 2\,\mathrm{fm}^{-1}$

# Deuteron as a nonrelativistic 2N bound state



$$\rho_d^0(\boldsymbol{r}') \propto C_0(2r') - 2C_2(2r')P_2(\cos\theta)$$
$$\rho_d^{\pm1}(\boldsymbol{r}') \propto C_0(2r') + C_2(2r')P_2(\cos\theta)$$
$$C_0(r) = {R_0}^2(r) + {R_2}^2(r)$$
$$C_2(r) = \sqrt{2}R_0(r)R_2(r) - \tfrac{1}{2}{R_2}^2(r)$$

($r' = r/2$ = distance from d CMS, $\theta$ = polar angle of $\boldsymbol{r}'$)

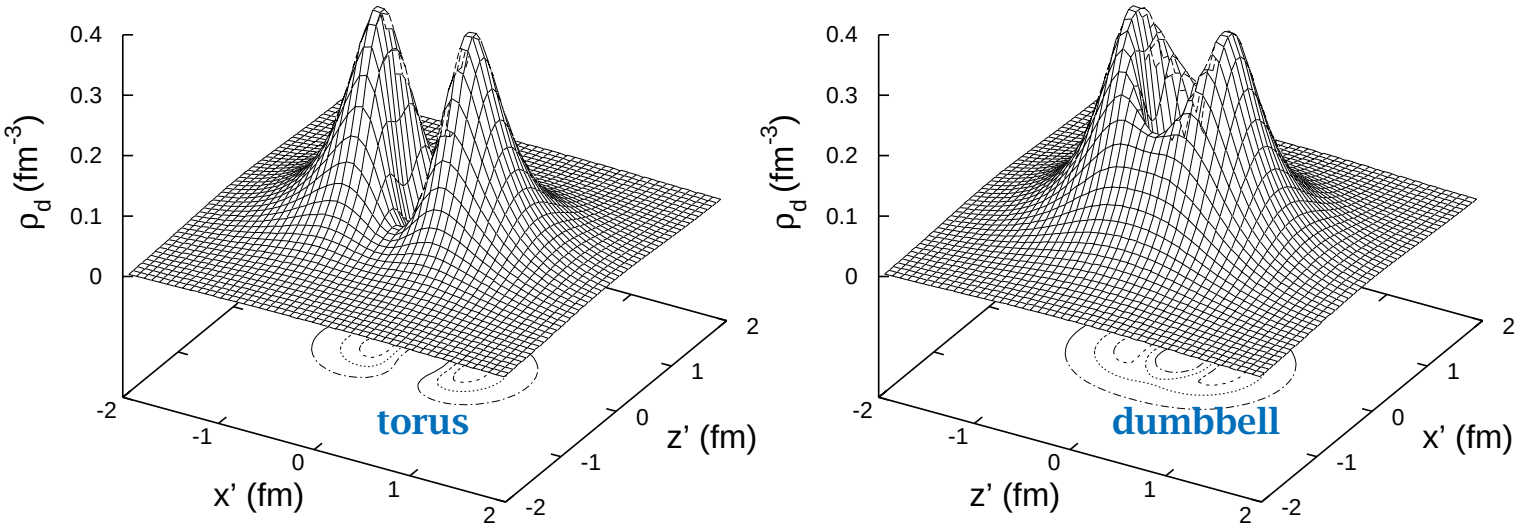


- $\rho_0 + \rho_1 + \rho_{-1}$ = sphere with radius $\propto R_0^2 + R_2^2$
- In absence of tensor force, $R_2 = 0 \implies \rho_0 = \rho_{\pm1}$
  $\implies$ Equidensity surfaces for $M_S = 0, \pm1$ are concentric spheres

Momentum-space wave-functions $u$ and $w$ for different NN potentials:

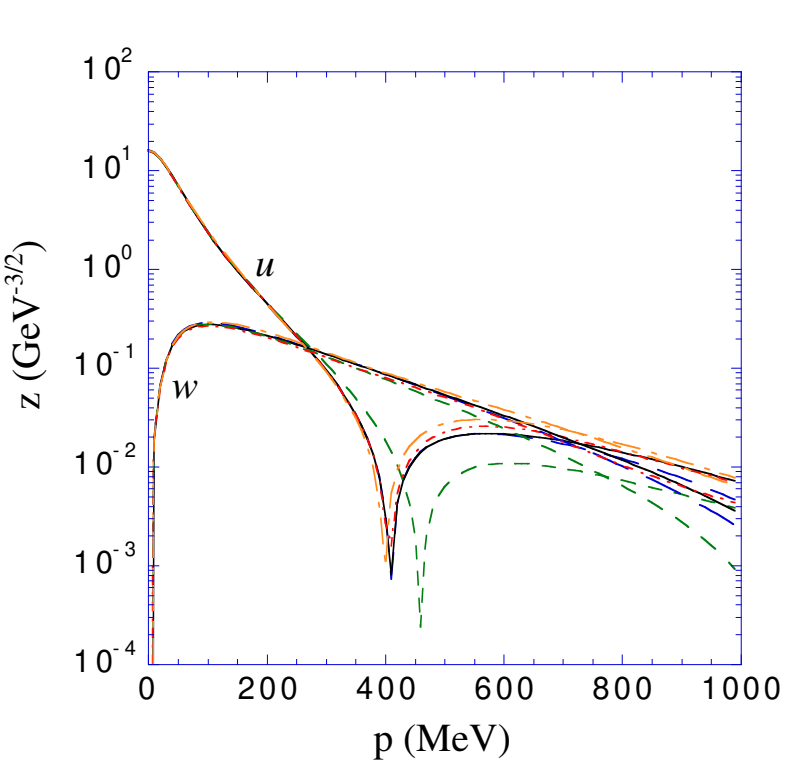


SCALED

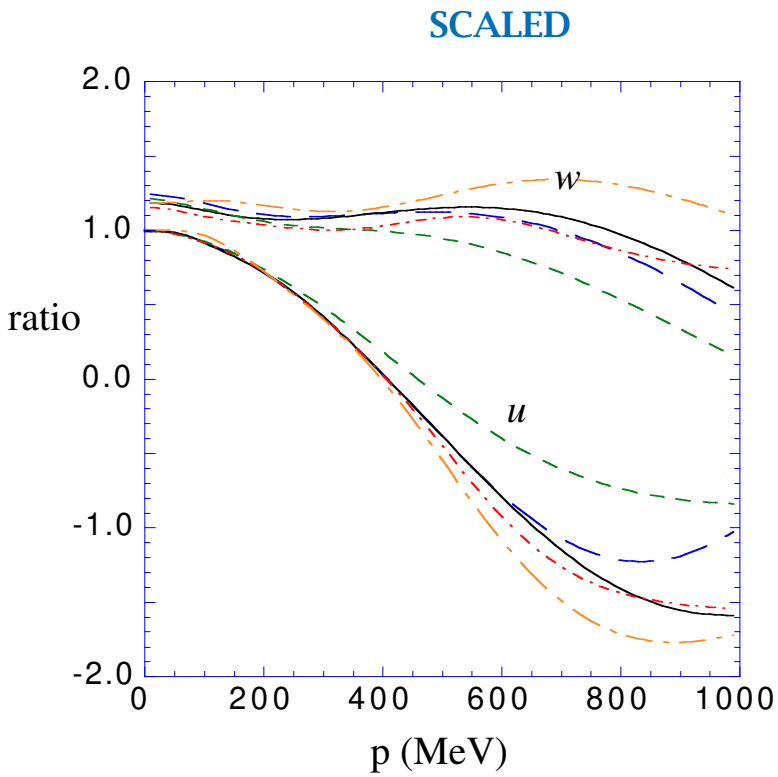


SCALED by functions which account for the bulk of $p$-dependence:

$$u_s(p) = \frac{16 m_N E_b}{(m_N E_b + p^2)(1 + p^2/p_0^2)}, \quad w_s(p) = \frac{16 m_N E_b p^2/p_1^2}{(m_N E_b + p^2)(1 + p^2/p_0^2)^2}$$

$E_b = 2.224\,\text{MeV}$, $p_0^2 = 0.15\,\text{GeV}^2$, $p_1^2 = 0.10\,\text{GeV}^2$

# Deuteron as a nonrelativistic 2N bound state



The resulting proton momentum distribution in deuteron:

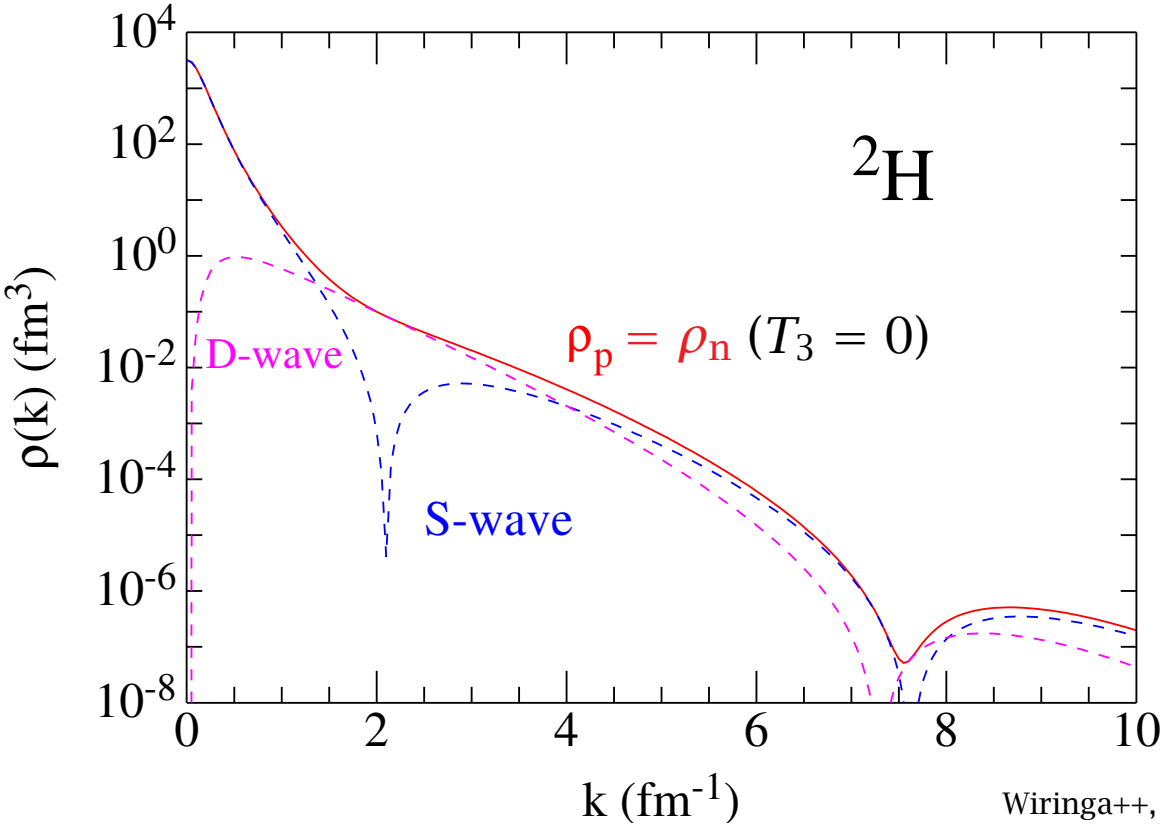


Wiringa++, PRC **89**, 024305 (2014)

- Prominent node in $S$-wave momentum density at $p \approx 2\,\mathrm{fm}^{-1}$
- Filled in by $D$-wave momentum density
- Broad shoulder out to $p \approx 7\,\mathrm{fm}^{-1}$, also a dominant feature in all single-nucleon momentum distributions in larger nuclei

# Exploiting the *D*-wave

With tensor polarization, $\rho_0$ and $\rho_{\pm 1}$ can be probed separately:

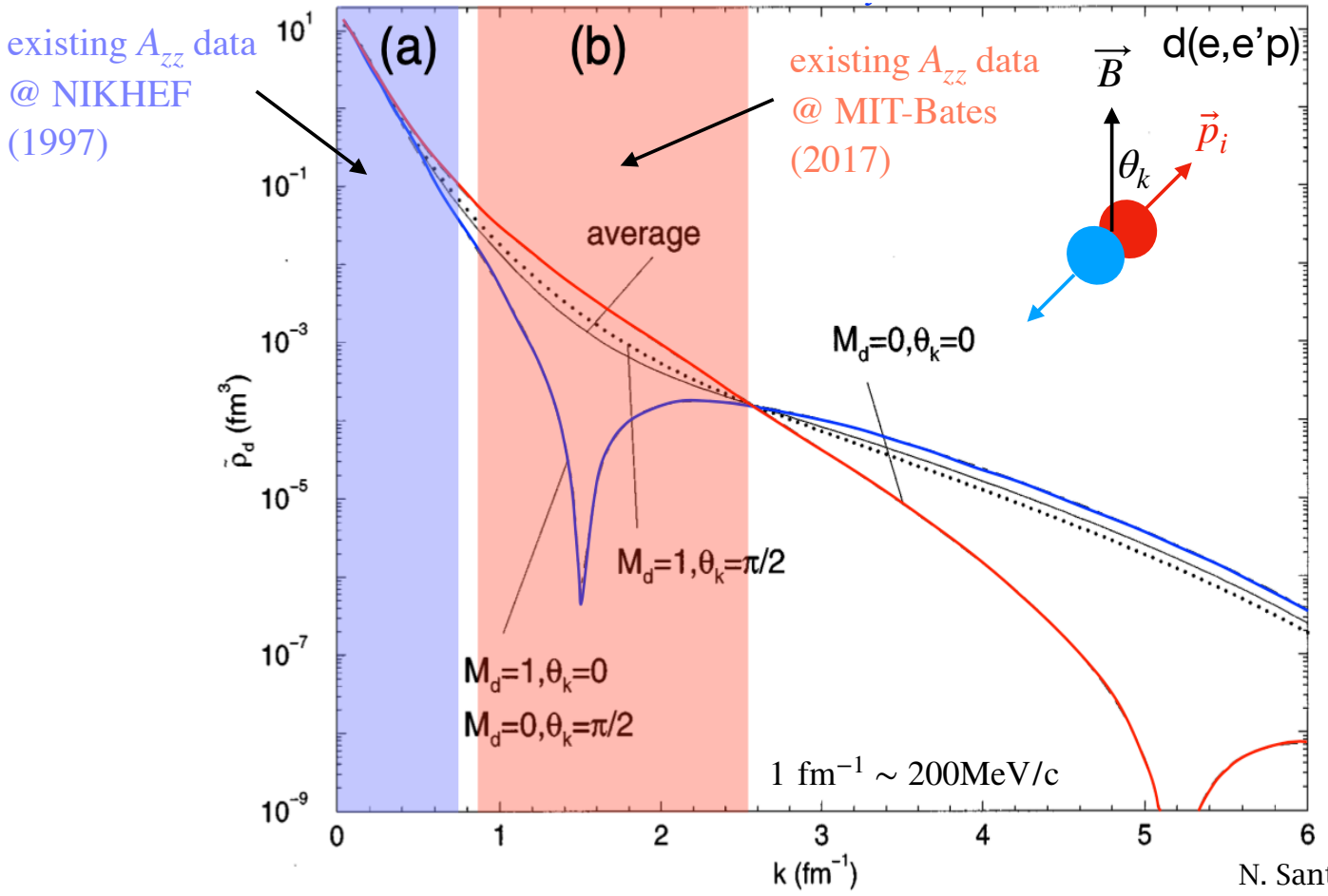


N. Santiesteban (Trento 2023)
based on Forest++, PRC **54**, 646 (1996)

(a) $p_{\text{miss}} \lesssim 0.75\,\text{fm}^{-1}$ covered by NIKHEF, shown later

(a), (b) $p_{\text{miss}} \lesssim 2.5\,\text{fm}^{-1}$ covered by MIT-Bates, shown later

# "How much" $D$-wave is there?

Wave-function asymptotics:

$$u(r) \sim A_S e^{-\alpha r} \qquad \text{as } r \to \infty$$

$$w(r) \sim A_D e^{-\alpha r}\left[1 + \frac{3}{\alpha r} + \frac{3}{\alpha^2 r^2}\right] \qquad \text{as } r \to \infty$$

$$\alpha = \sqrt{\tfrac{1}{2} E_b (M_n + M_p)} \approx 0.23161\,\text{fm}^{-1}$$

## Asymptotic $D/S$ ratio

$$\eta = A_D/A_S = \lim_{r\to\infty} \frac{w(r)}{u(r)} \approx 0.026$$

## $D$-state probability

$$P_D = \int_0^\infty w^2(r)\,\mathrm{d}r = (5 \pm 1)\,\%$$

- ▷ Precise value depends on choice of NN-potential
- ▷ Not a very rigorous parameter, but used in extracting information on the neutron by using the independent-particle approximation:

$$\mu_d \approx \mu_p + \mu_n - \frac{3}{2}\left(\mu_p + \mu_n - \frac{1}{2}\right) P_D$$

# Deuteron static properties



Mass — Determined by measurements of cyclotron frequency of various ions in Penning traps:

$$M_d = 1875.61294500(58)\,\mathrm{MeV}$$

CODATA 2022, Mohr++, RMP **97**, 025002 (2025)

Binding energy — Determined by measuring the energy of $\gamma$-rays from radiative p–n capture ($\mathrm{p} + \mathrm{n} \to \mathrm{d} + \gamma$) with thermal neutrons; $E_\gamma$, measured by a two-crystal spectrometer (Bragg) minus the recoil gives

$$E_b = 2.22456614(41)\,\mathrm{MeV}$$

Kessler++, PLA **255**, 221 (1999)

Size ("radius") — Determined by e–d or $\mu$–d scattering (EM), hadron–d scattering (strong) or spectroscopic methods (nuclear-dependent corrections to Lamb shift in H, D atoms)

$$r_{\mathrm{ch}}^2 \approx r_{\mathrm{m}}^2 + r_p^2 + r_n^2 + \frac{3}{4}\frac{1}{m_p^2}$$

**charge** **matter** **rel. corr.** (Darwin–Foldy)

$$r_{\mathrm{ch}} = \left( -6\,\frac{\mathrm{d}G_C}{\mathrm{d}Q^2}\bigg|_{Q^2=0} \right)^{1/2} = 2.12778(27)\,\mathrm{fm}\,, \quad r_{\mathrm{m}} \approx 1.95\,\mathrm{fm}$$

CODATA 2022 + · · ·

# Deuteron static properties



## Magnetic dipole moment

TABLE VI. *Deuterium.* $I_+'$ is the current to focus $+f_3$, and $I_-'$ is the current to focus $-f_3$. $I_A=(I_+'+I_-')/2$. Currents in amperes.

| *B* Field Current $I''$ | *A* Field Current $I_+'$ | $I_-'$ | $I_A$ | $\mu_D$ |
|---|---|---|---|---|
| 349 | 66.3 | 73.2 | 69.7 | 0.854 |
| 400 | 68.2 | 78.8 | 73.5 | .841 |
| 440 | 72.4 | 82.4 | 77.4 | .848 |

These measurements yield for the proton moment a value of 2.85±0.15 nuclear magnetons; and for the deuteron a value of 0.85±0.03 nuclear magnetons. Our judgment of the precision comes from a discussion of the possible errors in the determination of the geometry.

$$\mu_p = (2.85 \pm 0.15)\,\mu_N$$
$$\mu_d = (0.85 \pm 0.15)\,\mu_N$$

Kellogg++, PR **50**, 472 (1936)

$$\mu_d = 0.8574382335(22)\,\mu_N$$

CODATA 2022, Mohr++, RMP **97**, 025002 (2025)

## Electric quadrupole moment

To prove that the large displacements in $D_2$ are of nuclear origin rather than molecular, similar experiments were performed on the proton and the deuteron in the HD molecule. The group of resonance minima for H was narrow as expected and that for D had large displacements as in $D_2$. Furthermore, the experimentally evaluated spin-orbit interaction constant for $D_2$ is one-half as great as that for $H_2$ as predicted. We therefore believe that the apparent large spin-spin interaction is not magnetic, nor is it of molecular origin and must be a nuclear effect which behaves like a quadrupole moment.

To obtain the magnitude of this quadrupole moment one must know the molecular electric field. This value can be calculated from the various wave functions which have been suggested for the hydrogen molecule. The result of such a calculation by Dr. A. Nordsieck with Wang wave functions when combined with our data yields a quadrupole moment $Q=(3z^2-r^2)_{Av}$ of about $2\times10^{-27}$ cm². The chief source of error lies in the inaccuracy of the wave functions.

$$Q_d \approx 0.2\,\mathrm{fm}^2$$

Kellogg++, PR **55**, 318 (1939); PR **57**, 677 (1940)

$$Q_d = 0.285783(30)\,\mathrm{fm}^2$$

Pavanello++, PRA **81** (2010) 042526

$$Q_d = 0.285699(15)(18)\,\mathrm{fm}^2$$

Puchalski++, PRL **125** (2020) 253001

# Dealing with ensembles of spin–1 particles

In an experiment (= in a target), deuterons with $s = 1$, $-s \le s_z = m \le s$, form a statistical ensemble, i.e. an incoherent mixture of pure states $|\psi^{(i)}\rangle$, each with probability $p^{(i)}$, $\sum_i p^{(i)} = 1$, and with expansion

$$|\psi^{(i)}\rangle = \sum_{m=-1}^{1} c_m^{(i)} |1m\rangle$$

Statistical mixture of magnetic substates $\Longrightarrow$ spin density matrix

The expectation value of arbitrary operator $\hat{A}$:

$$\langle \hat{A} \rangle = \sum_{mm'} A_{m'm} \rho_{mm'} = \mathrm{tr}[A\rho]$$

where

$$A_{m'm} = \langle sm'|\hat{A}|sm\rangle$$
$$\rho_{mm'} = \sum_i p^{(i)} c_m^{(i)} c_{m'}^{(i)*}$$

matrix elements of density matrix in $|1m\rangle$ basis

- Dynamics: $\dot{\rho}(t) = -(\mathrm{i}/\hbar)[H, \rho(t)]$, solved by $\rho(t) = \mathrm{e}^{-\mathrm{i}Ht/\hbar}\rho(0)\mathrm{e}^{\mathrm{i}Ht/\hbar}$
- $\rho_{mm} \ge 0 \; \forall m$ | $\mathrm{tr}[\rho] = 1$ | $\rho$ is hermitian, hence diagonalizable
- $\rho$ fully specified by $(2s+1)^2 - 1$ real parameters

# The spin–1 density matrix



In terms of expectation values of rank–0, 1 and 2 tensor operators:

$$\rho = \frac{1}{3}\sum_{LM}(2L+1)t_M^{L\star}T_M^L = \frac{1}{3}\left[t_0^{0\star}T_0^0 + 3\sum_{M=-1}^{1} t_M^{1\star}T_M^1 + 5\sum_{M=-2}^{2} t_M^{2\star}T_M^2\right]$$

$T_M^L = \langle sm|\hat{T}_M^L|sm'\rangle$, where $\hat{T}_0^0 = 1$, $\hat{T}_0^1 = \hat{s}_z/\sqrt{2}$, $\hat{T}_{\pm1}^1 = \mp(\hat{s}_x \pm \mathrm{i}\hat{s}_y)/2$, etc. In Cartesian form:

$$\rho = \frac{1}{3}\left[I + \frac{3}{2}\boldsymbol{P}\cdot\boldsymbol{S} + \sqrt{\frac{3}{2}}\sum_{ij} T_{ij}\left(S_iS_j + S_jS_i - \frac{4}{3}\delta_{ij}I\right)\right]$$

Matrix representations of spin operators $\hat{s}_i$:

$$S_x = \frac{1}{\sqrt{2}}\begin{pmatrix}0&1&0\\1&0&1\\0&1&0\end{pmatrix}, \quad S_y = \frac{\mathrm{i}}{\sqrt{2}}\begin{pmatrix}0&-1&0\\1&0&-1\\0&1&0\end{pmatrix}, \quad S_z = \begin{pmatrix}1&0&0\\0&0&0\\0&0&1\end{pmatrix}$$

- $\boldsymbol{P} = \langle\hat{\boldsymbol{s}}\rangle \longleftarrow$ polarization vector, **3** components
- $T_{ij} = \frac{1}{2}\sqrt{\frac{3}{2}}\left(\langle\hat{s}_i\hat{s}_j + \hat{s}_j\hat{s}_i\rangle - \frac{4}{3}\delta_{ij}\right) \longleftarrow$ rank–2 tensor, **5** independ. components

$$t_0^0 = 1\,, \quad t_0^1 = \frac{1}{\sqrt{2}}P_z\,,\ t_{\pm1}^1 = \cdots\,, \quad t_0^2 = \sqrt{\frac{3}{5}}T_{zz}\,,\ t_{\pm1}^2 = \cdots\,,\ t_{\pm2}^2 = \cdots$$

# The spin–1 density matrix 2

- In a frame where $z$-axis is along the quantization direction, $\rho$ is diagonal and $t_M^L = 0 \; \forall M \neq 0$
- spin 1/2: quantization axis (QA) is along $\boldsymbol{P}$
- spin 1: QA becomes a more general concept since one can have zero vector polarization yet still maintain some sort of "alignment" along the QA
- An ensemble of $N$ deuterons has $(N_+, N_0, N_-)$ particles in magnetic substates $m = +1, 0, -1$ with probabilities $(p_+, p_0, p_-)$, where $N_+ + N_0 + N_- = N$ and $p_+ + p_0 + p_- = 1$
- The density matrix then has the form

$$\rho = \frac{1}{3} I + \frac{1}{2} P_z S_z + \frac{1}{6} P_{zz} (3 S_z^2 - 2I)$$

Vector polarization:

$$-1 \leq P_z = \frac{N_+ - N_-}{N} \leq 1$$

Tensor polarization (also known as *alignment*):

$$-2 \leq P_{zz} = \frac{N_+ + N_- - 2N_0}{N} = \frac{N - 3N_0}{N} \leq 1$$

# Achieving nuclear polarization

The behavior of the deuteron ensemble in magnetic and electric fields — and hence its **polarization** — is driven by effects on $\mu_d$ and $Q_d$

## Two traditional techniques to achieve nuclear polarization

- Dynamical Nuclear Polarization (DNP)
  - ▷ Use appropriate RF irradiation, NMR for diagnostics
  - ▷ Density-matrix formalism with appropriate Boltzmann weights
- Exploiting hyperfine interactions (atomic beam sources, ABS)
  - ▷ Manipulate combined nuclear/electronic levels to obtain desired nuclear population, use *electron* (Breit-Rabi) or ion polarimetry for diagnostics

## Both need external $\boldsymbol{B}$ (Zeeman) to attain and maintain

# Deuteron energy levels in external EM fields

Driven by $\mu_d$ via Zeeman splittings, compounded by effects of $Q_d$:

$$E_m = -m\hbar\omega_D + \hbar\omega_Q[(3\cos^2\theta - 1) + \eta\sin^2\theta\cos 2\phi](3m^2 - 2)$$

$$\hbar\omega_D = \mu_d B_z$$

$$\hbar\omega_Q \propto Q_d \cdot \text{electric field gradient(EFG)}$$

$\theta$ = angle between $\boldsymbol{B}$ and EFG

$\phi$, $\eta$ = needed when EFG not symmetric about the bond axis

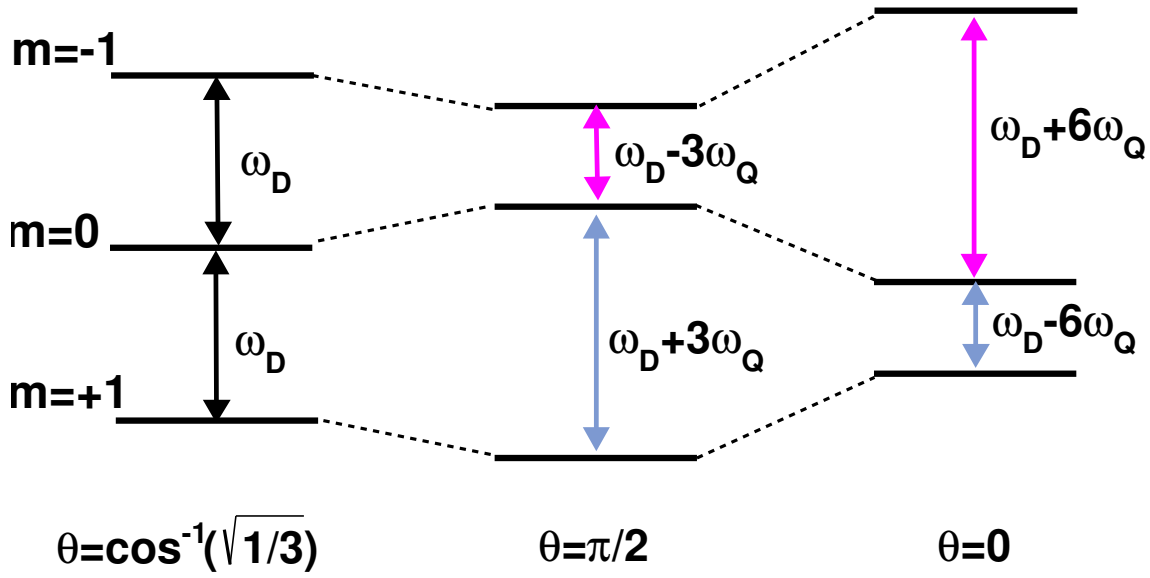


(Splittings not to scale)

Keller, EPJA **53**, 155 (2017)

# Example: Dynamic nuclear polarization in $ND_3$

Typical NMR signal showing the superposition of $I_+$ and $I_-$ lineshapes:

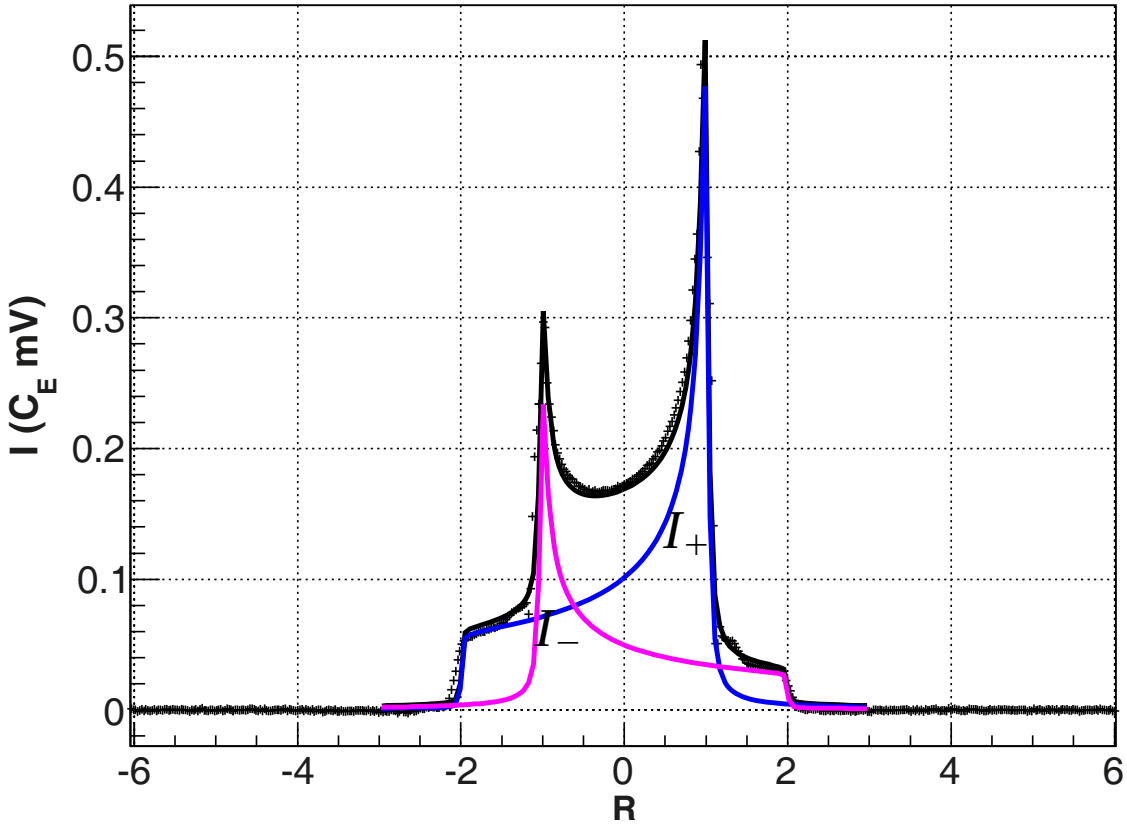


$P_z = 42.3\,\%$, $P_{zz} = 13.1\,\%$

Keller, EPJA **53**, 155 (2017)

- External [high-density] polarized targets use DNP
- Internal [low-density] targets (within storage rings) have used ABS
  Two historic facilities: AmPS @ NIKHEF and MIT–Bates

# AmPS at NIKHEF

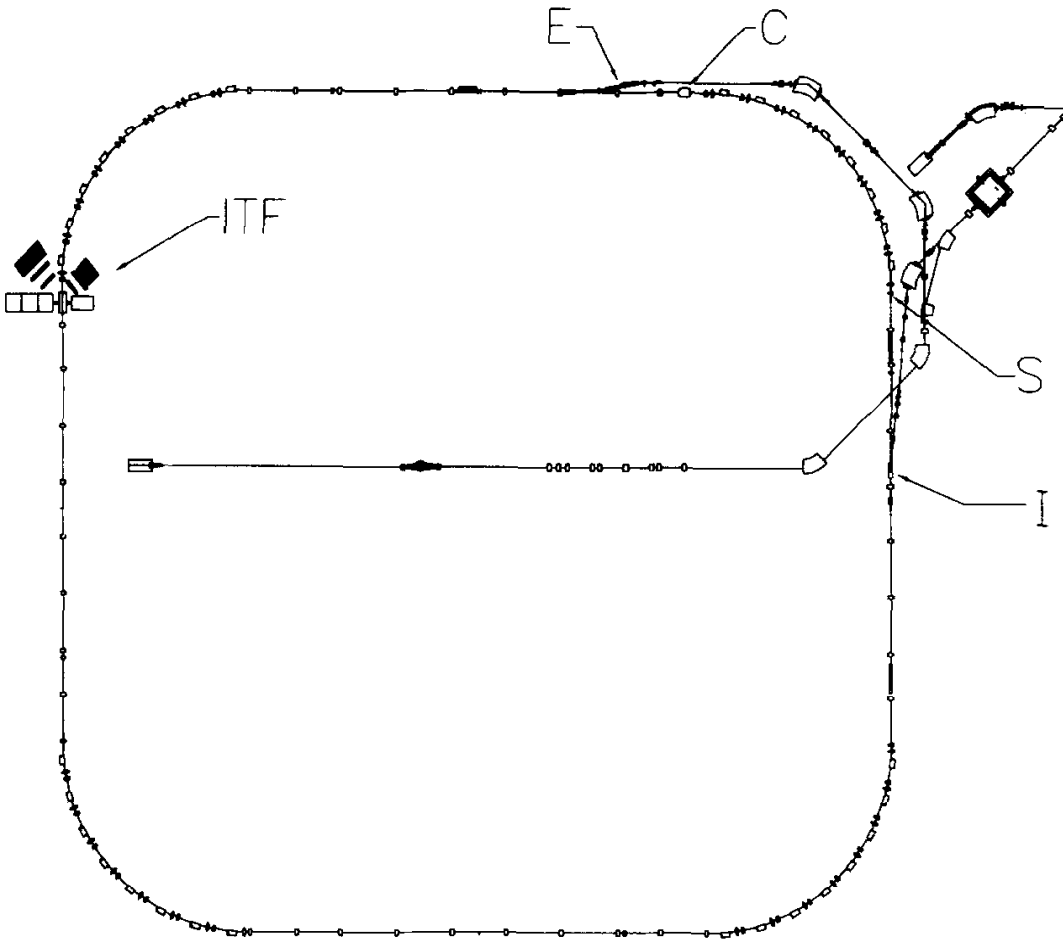


MEA = Medium Energy electron accelerator (up to 700 MeV)

C = 476 MHz cavity to compensate for synchrotron radiation loss

$\Longrightarrow$ $\approx$ 15 min beam lifetimes

565 MeV energy

$\lesssim$ 120 mA currents

100 % duty factor

ITF = Internal Target Facility

E = Extraction line (for EMIN)

polarized beam after mid-1990s

Zhou++, NIMA **378**, 40 (1996)

# Accelerator / Experiment Layout at MIT–Bates

Pre-BLAST era:
— Elssy
— MEPS
— SAMPLE
— OOPS + OHIPS (extracted beam)

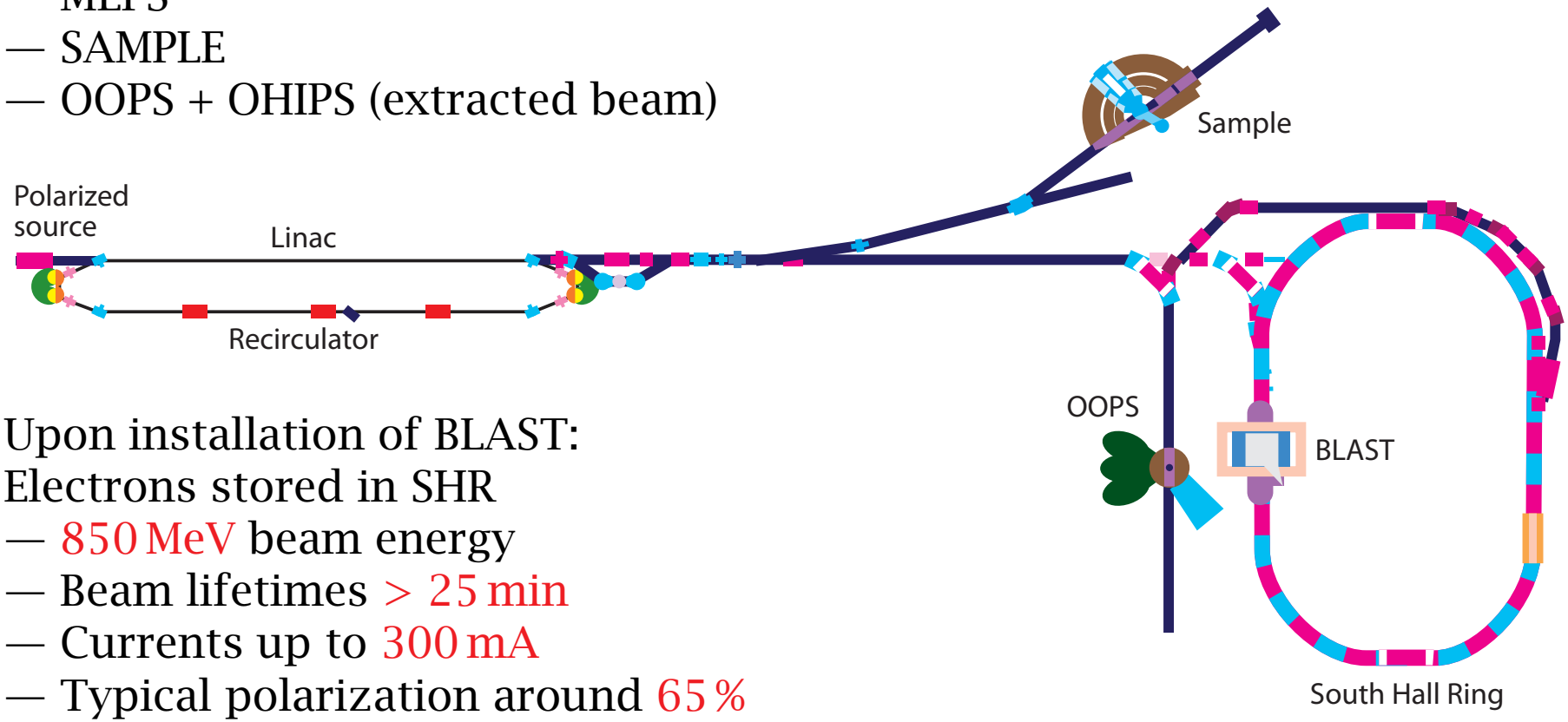


Upon installation of BLAST:
Electrons stored in SHR
— 850 MeV beam energy
— Beam lifetimes > 25 min
— Currents up to 300 mA
— Typical polarization around 65 %
Longitudinal orientation at target maintained by “Siberian snake”
Polarization monitored by Compton polarimeter

Hasell++, NIMA **603**, 247 (2009)
Morozov++, PRSTAB **4**, 104002 (2001)

# First detector setup in ITF @ NIKHEF

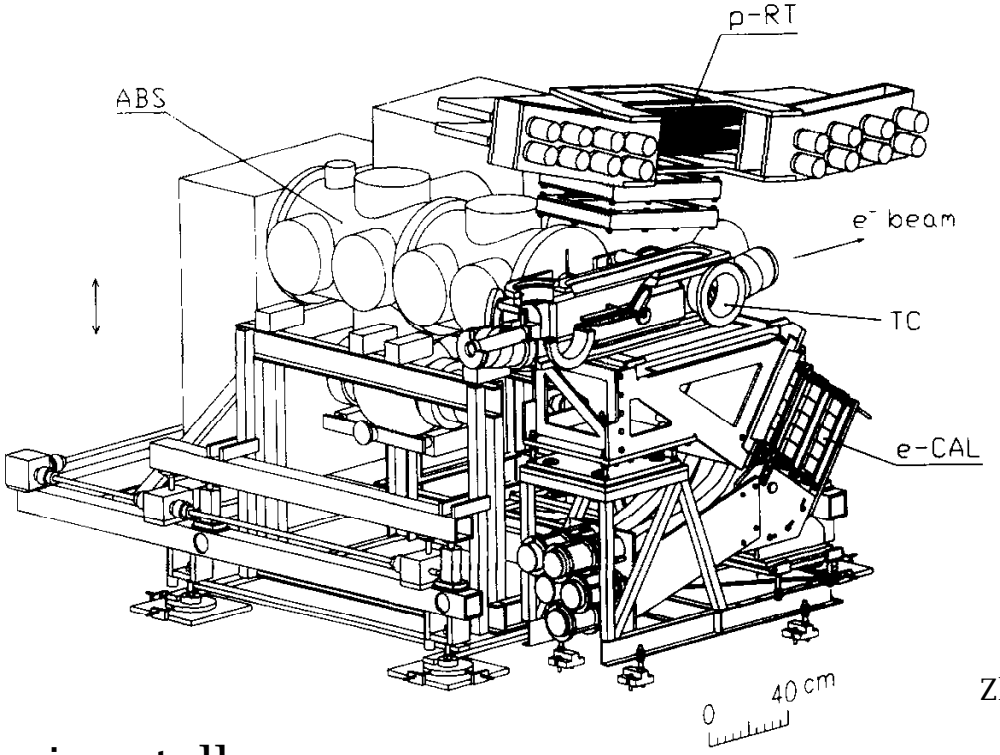


Zhou++, NIMA **378**, 40 (1996)

- ABS mounted horizontally
- Electrons: EM calorimeter = 6 layers of CsI(Tl) blocks,
  +2 plastic scintillators for triggering, $\Delta\Omega = 180\,\text{msr}$, $\delta E \approx 22\,\text{MeV}$
- Hadrons: range telescope = $1 \times 2$ mm + $15 \times 1$ cm plastic scintillator
  +2 sets of VDCs for tracking, $\Delta\Omega \approx 300\,\text{msr}$, $E^d_{\text{thr}} = 19\,\text{MeV}$
- Used for $T_{20}$ in elastic $^2\overleftrightarrow{\text{H}}\,(\text{e},\text{e}')$
  and $A_{\text{d}}^{\text{T}}$ in QE $^2\overleftrightarrow{\text{H}}\,(\text{e},\text{e}'\text{p})$

# NIKHEF setup with BigBite

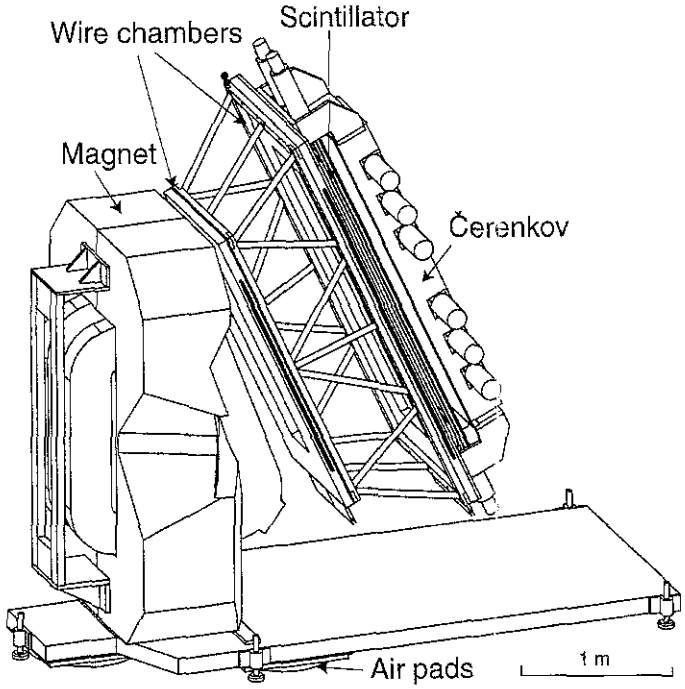


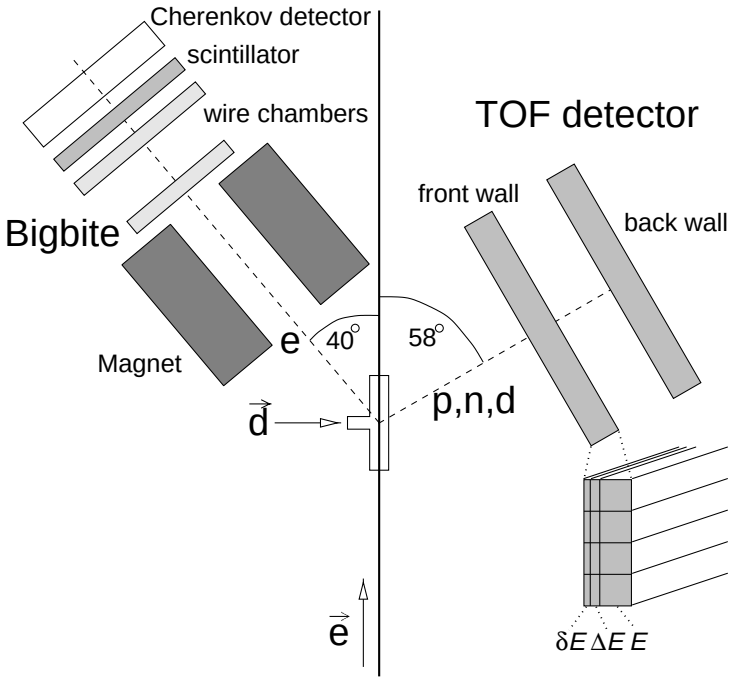


de Lange++, NIMA **406**, 182 (1998); NIMA **412**, 254 (1998)
Higinbotham, NIMA **414**, 332 (1998)

- Electrons: NIKHEF incarnation of BigBite: $\Delta\Omega = 96$ msr, $250 \leq p \leq 720$ MeV/$c$
- Hadrons: ToF system = 2 arrays of segmented (20 cm) plastic scintillators:
  "$\delta E$"/3 mm + "$\Delta E$"/10 mm (veto) + "$E$"/20 cm
- Used for $A_{ed}^{v}$ in QE $^2\vec{H}(\vec{e}, e'n) \Longrightarrow G_E^n$
  and $A_{ed}^{v}$ in QE $^2\vec{H}(\vec{e}, e'p)$

# The BLAST Detector @ MIT–Bates

- Toroidal field, 8 normal conducting coils, max. 3.8 kGauss
- Only 1/6 azimuth instrumented
  - ▷ VDCs: $\pm 15^\circ$ in $\phi$, L and R, $20^\circ \lesssim \theta \lesssim 80^\circ$
  - ▷ Aerogel Cherenkov detectors for e|$\pi$: $n = 1.020, 1.030$; $\varepsilon \approx 90\,\%$
  - ▷ ToF scintillators: BC-408
  - ▷ Neutron detectors ("Ohio walls", LADS15, LADS20 in variable configuration): BC-408

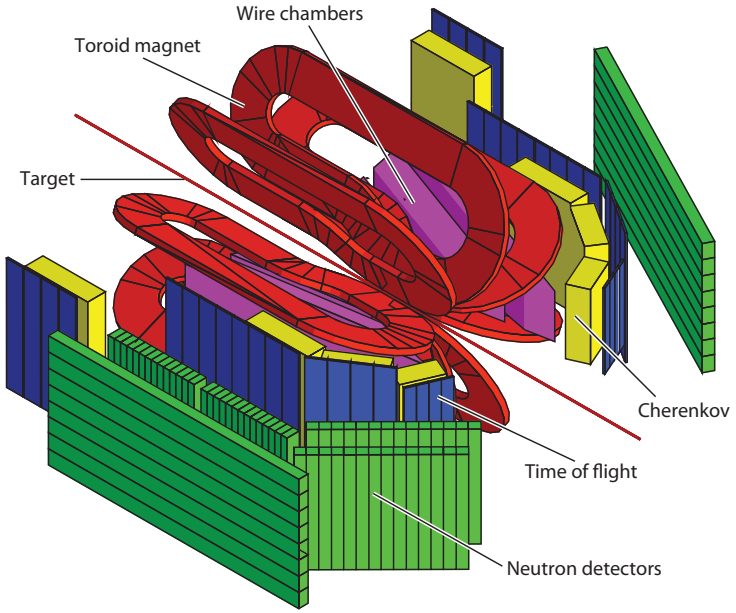


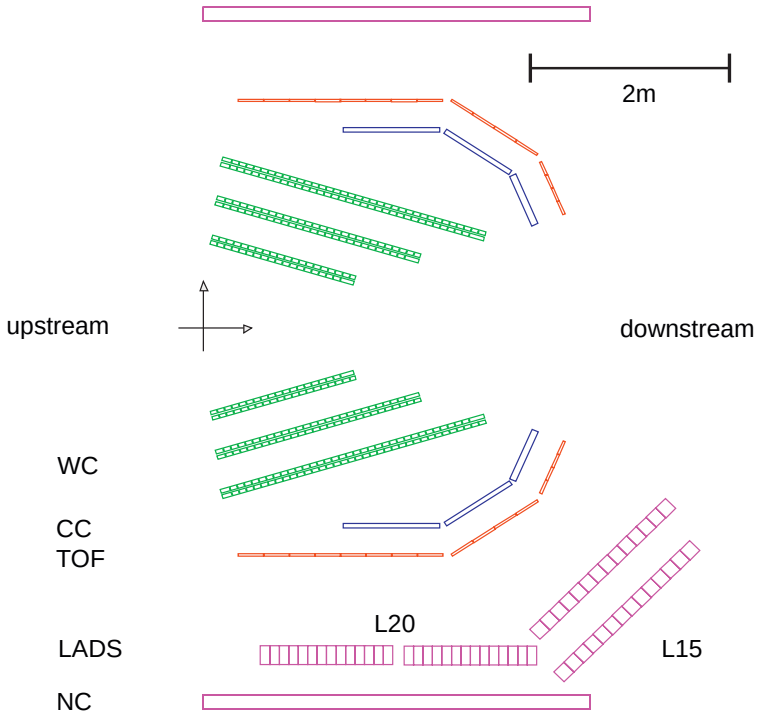


Hasell++, NIMA **603**, 247 (2009)

# The heart of both setups: the ABS = Atomic Beam Source

- Exploits [transitions between] hyperfine states of deuterium atoms
- Interaction Hamiltonian of coupled nuclear ($\vec{I}$) and electron ($\vec{J}$) spins:

$$H_{\text{int}} = \mu_{\text{B}} \left( g_I \vec{I} + g_J \vec{J} \right) \cdot \vec{B} + \frac{2h\nu_0}{3} \vec{I} \cdot \vec{J}$$

$g_I = -0.00047$
$g_J = 2.0023$
$h\nu_0 = \mu_{\text{B}}(g_J - g_I)B_{\text{c}}$
$B_{\text{c}} = 11.7\,\text{mT}$
$\nu_0 = 327.4\,\text{MHz}$

- Energy eigenstates = linear combinations of spin eigenstates:

$$\begin{aligned}
|1\rangle &= |1, \tfrac{1}{2}\rangle \\
|2\rangle &= \alpha_{-+}|1, -\tfrac{1}{2}\rangle + \alpha_{++}|0, \tfrac{1}{2}\rangle \\
|3\rangle &= \alpha_{--}|0, -\tfrac{1}{2}\rangle + \alpha_{+-}|-1, \tfrac{1}{2}\rangle \\
|4\rangle &= |-1, -\tfrac{1}{2}\rangle \\
|5\rangle &= \alpha_{+-}|0, -\tfrac{1}{2}\rangle - \alpha_{--}|-1, \tfrac{1}{2}\rangle \\
|6\rangle &= \alpha_{++}|1, -\tfrac{1}{2}\rangle - \alpha_{-+}|0, \tfrac{1}{2}\rangle
\end{aligned}$$

$\alpha_{+\pm} = \sqrt{\frac{1}{2}(1 + a_\pm)}$
$\alpha_{-\pm} = \sqrt{\frac{1}{2}(1 - a_\pm)}$
$a_\pm = (x \pm \frac{1}{3})/\sqrt{1 \pm \frac{2}{3}x + x^2}$
$x = B/B_{\text{c}}$

- Vector/tensor polarizations (ensemble averages):

$$\begin{aligned}
P_z &= \langle I_z \rangle = n_1 + \alpha_{-+}^2 n_2 - \alpha_{+-}^2 n_3 - \alpha_{--}^2 n_5 + \alpha_{++}^2 n_6 = n_+ - n_- \\
P_{zz} &= \langle 3I_z^2 - 2 \rangle = 1 - 3\left( \alpha_{++}^2 n_2 + \alpha_{--}^2 n_3 + \alpha_{+-}^2 n_5 + \alpha_{-+}^2 n_6 \right) = 1 - 3n_0
\end{aligned}$$

# Hyperfine transitions in deuterium, $P_z$ and $P_{zz}$

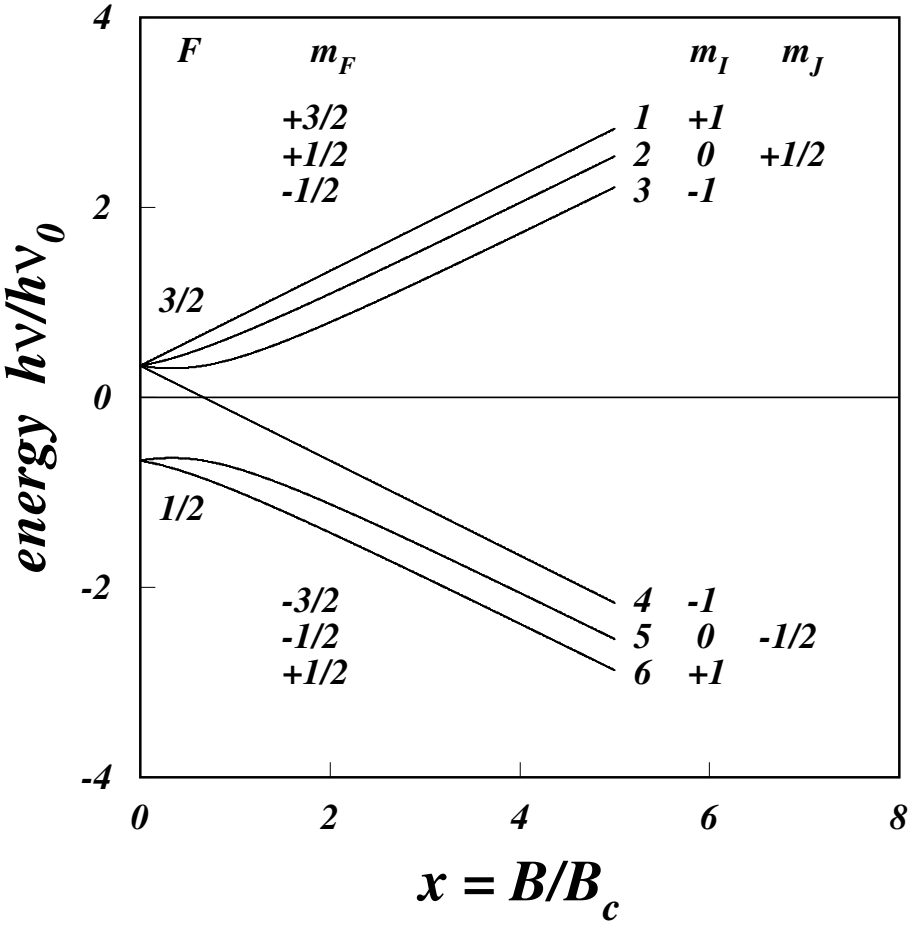


$$\vec{F} = \vec{I} + \vec{J}$$

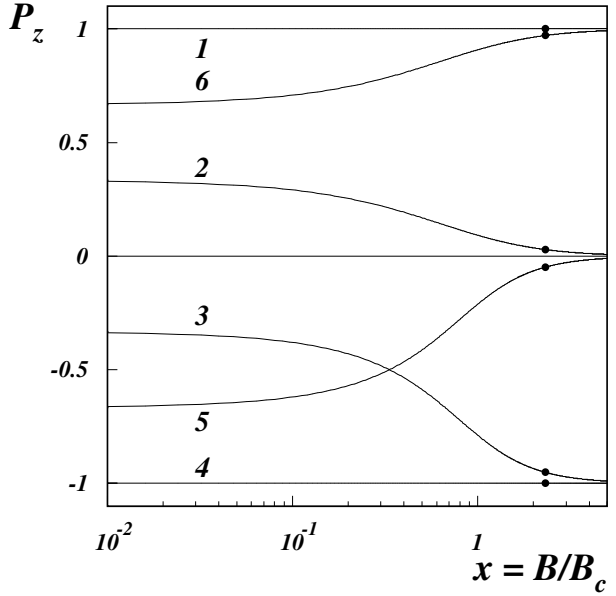


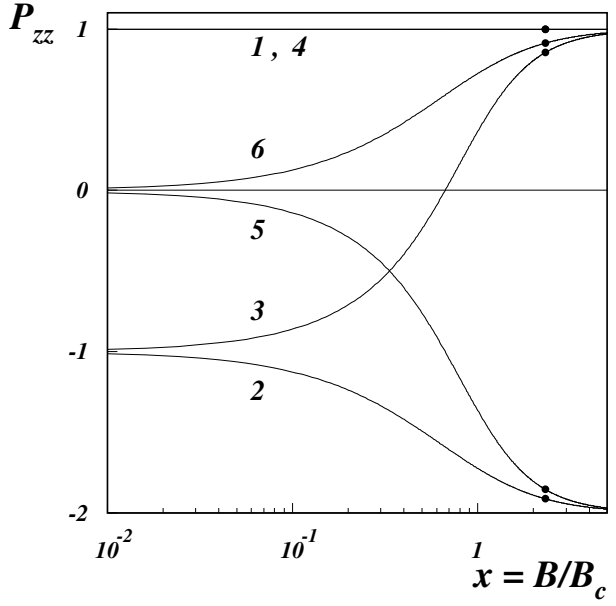

# ABS setup at NIKHEF and MIT-Bates

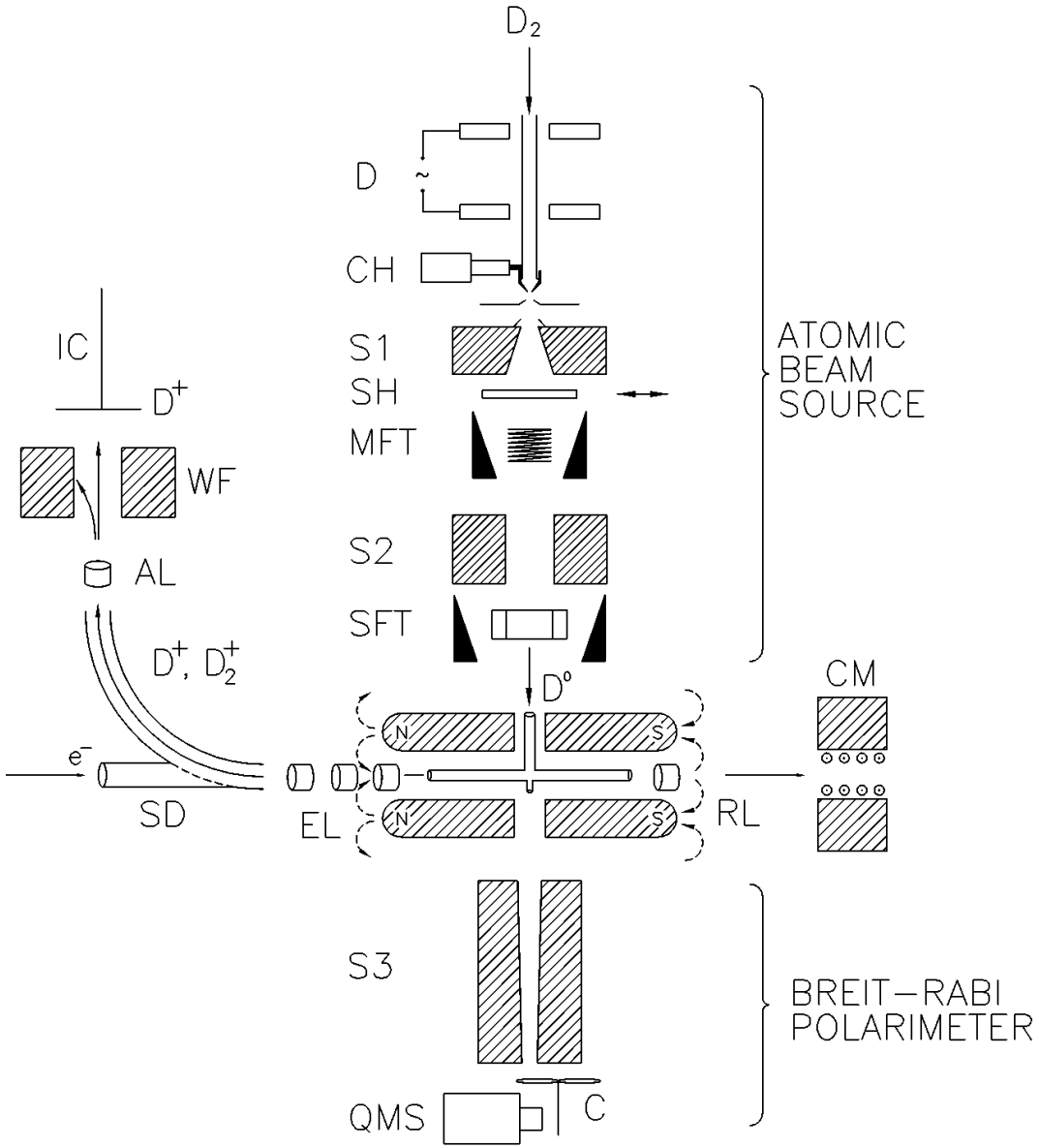


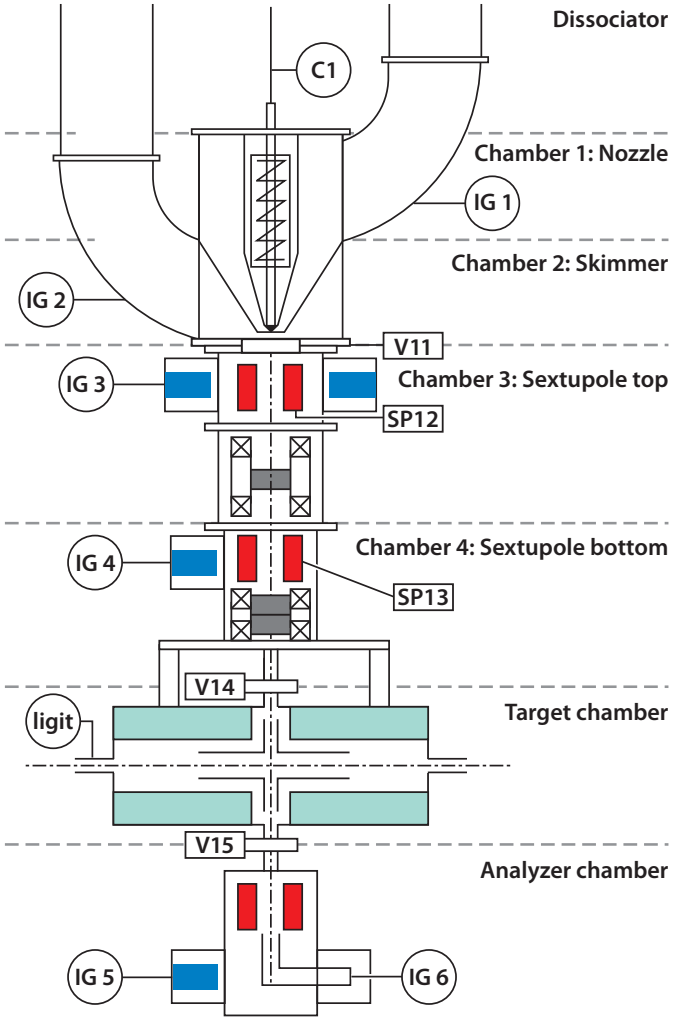

# The internal target (storage cell)

- Storage cell design increases luminosity by 2–3 orders of magnitude wrt. free atomic beam (jet) without compromising the electron beam passing through
- Density has approximately triangular shape (can be mapped well)
- Orientation of nuclear polarization maintained by holding field, $B \approx 30\,\mathrm{mT}$

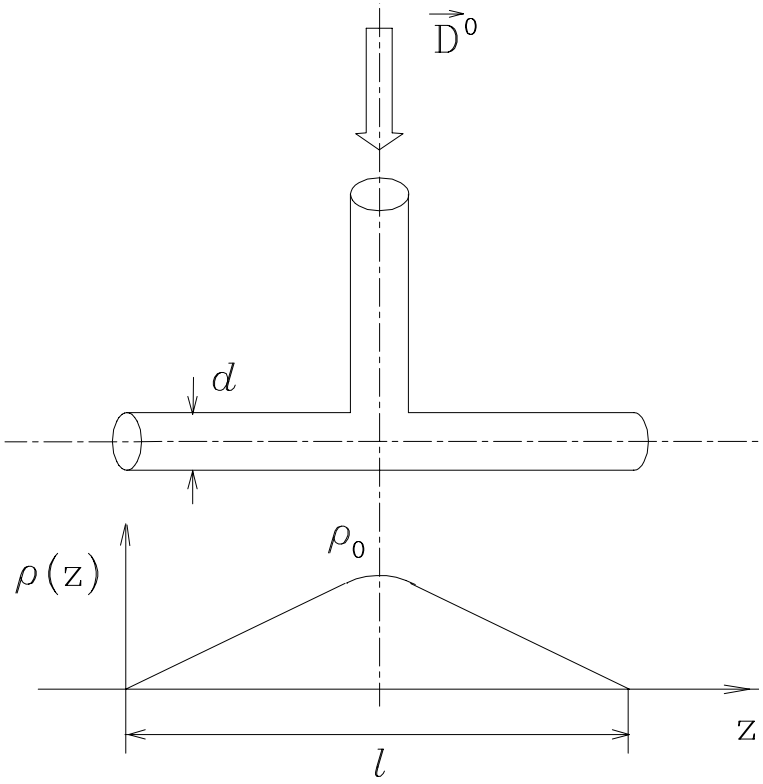


▷ $\mathcal{L} \propto \dfrac{l^2}{d^2}\dfrac{1}{\sqrt{T_{\mathrm{cell}}}}$

$l = 40\,\mathrm{cm}$, $d = 1.5\,\mathrm{cm}$, $T_{\mathrm{cell}} = 100\,\mathrm{K}$

typical $\mathcal{L} \approx 10^{31}$—$10^{32}\,\mathrm{cm}^2/\mathrm{s}$

typical atomic beam intensity $\approx 10^{16}/\mathrm{s}$

(can be tweaked by $T_{\mathrm{nozzle}}$ and gas admixtures)

▷ $t_{\mathrm{dwell}} = t_{\mathrm{flight}} + N_{\mathrm{coll}} t_{\mathrm{stick}}$

$t_{\mathrm{flight}} \propto \dfrac{l^2}{d}\sqrt{T_{\mathrm{cell}}}$

$t_{\mathrm{flight}} \approx 4\,\mathrm{ms}$

$N_{\mathrm{coll}} = 270$, $N_{\mathrm{coll}} t_{\mathrm{stick}} \approx 10^{-9}\,\mathrm{s} \ll t_{\mathrm{flight}}$

# ABS — the RF transition schemes

| | Tensor ($B_t \gg 11.7$ mT) | | Vector ($B_t \gg 11.7$ mT) | | Vector ($B_t \ll 11.7$ mT) | |
|---|---|---|---|---|---|---|
| | + | − | + | − | + | − |
| States after $1^{st}$ sext. | 1 , 2 , 3 | | 1 , 2 , 3 | | 1 , 2 , 3 | |
| MFT | $1 \leftrightarrow 4$ | | $3 \leftrightarrow 4$ | | $3 \leftrightarrow 4$ | |
| States after MFT | 2 , 3 , 4 | | 1 , 2 , 4 | | 1 , 2 , 4 | |
| States after $2^{nd}$ sext. | 2 , 3 | | 1 , 2 | | 1 , 2 | |
| SFT | $2 \leftrightarrow 6$ | $3 \leftrightarrow 5$ | $2 \leftrightarrow 6$ | off | $2 \leftrightarrow 6$ | |
| States after SFT | 3 , 6 | 2 , 5 | 1 , 6 | 1 , 2 | 1 , 6 | |
| WFT | off | | off | $1,2 \leftrightarrow 3,4$ | off | $1,6 \leftrightarrow 5,4$ |
| States after WFT | 3 , 6 | 2 , 5 | 1 , 6 | 3 , 4 | 1 , 6 | 4 , 5 |
| Tensor Polariz. $P_{zz}$ | +1 | −2 | +1 | +1 | +1/2 | +1/2 |
| Vector Polariz. $P_z$ | 0 | 0 | +1 | −1 | +5/6 | −5/6 |
| Figure of merit | 18 | | 8 | | 5.6 | |

# Typical performance of ABS

NIKHEF

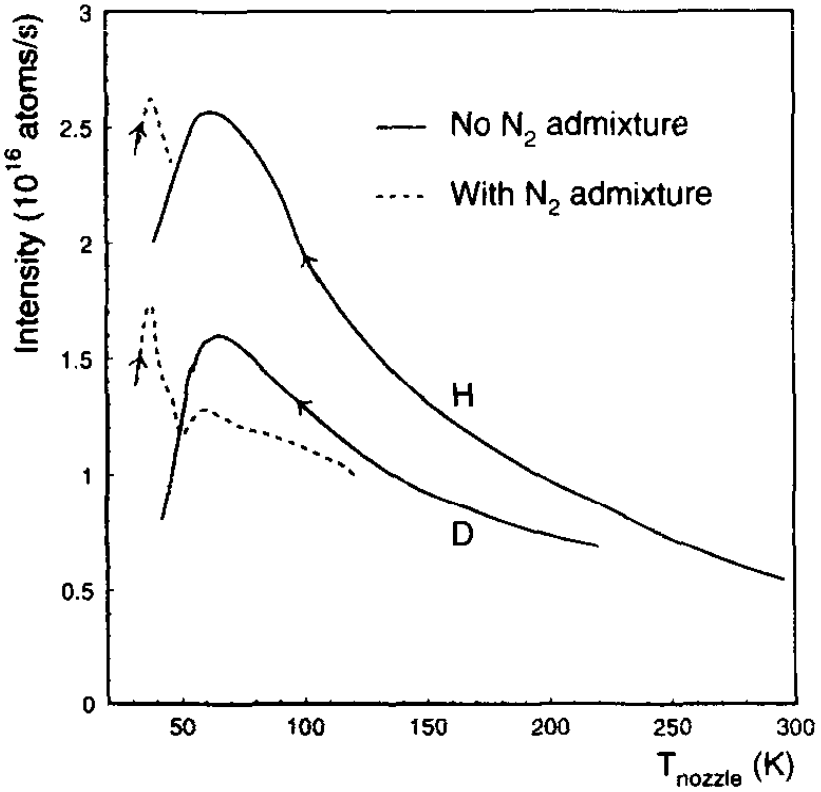


MIT-Bates

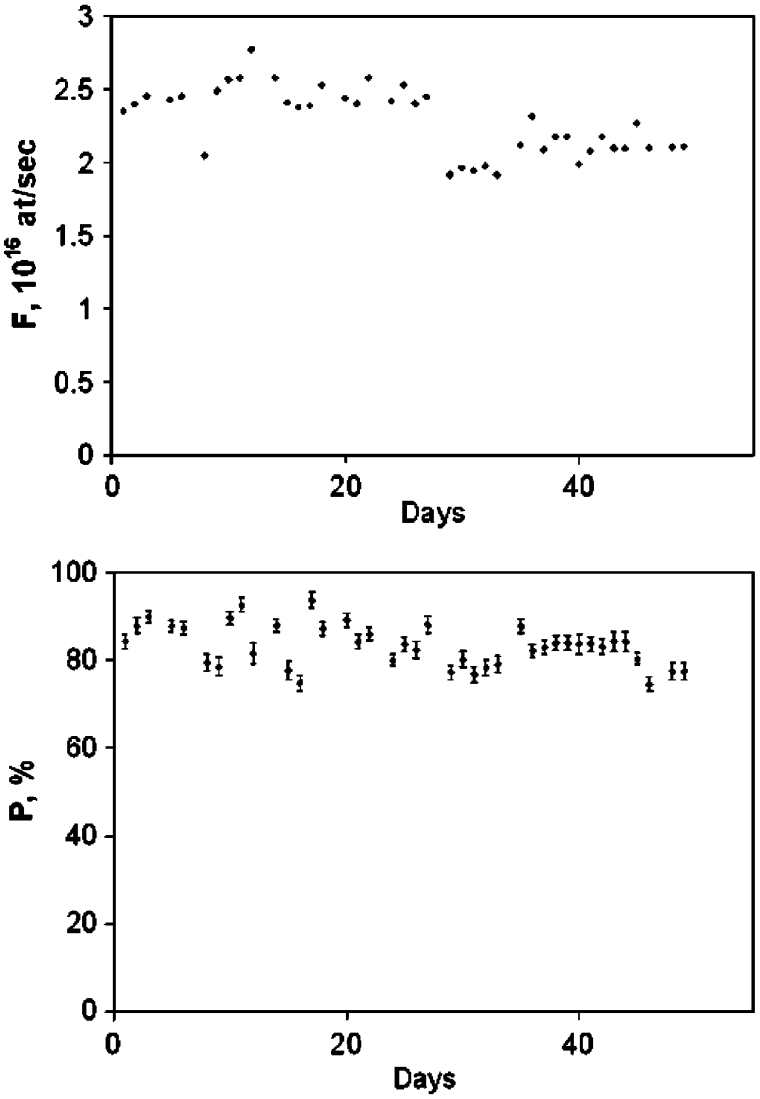


Cheever++, NIMA **556**, 410 (2006)

# Target polarimetry #1

## Breit-Rabi electron polarimeter

- The 1–4, 2–6 and 3–5 RF transitions involve a *collective* electron and nuclear spin flip
  $\Longrightarrow$ a measurement of electronic polarization allows one to measure the efficiencies of the MFT and SFT, and control the injected polarization states

- Typical efficiencies:
  $\varepsilon(1 \leftrightarrow 4) = 0.97 \pm 0.01$
  $\varepsilon(2 \leftrightarrow 6) = 1.02 \pm 0.02$
  $\varepsilon(3 \leftrightarrow 5) = 0.99 \pm 0.02$

Ferro-Luzzi++, NIMA **364**, 44 (1995)

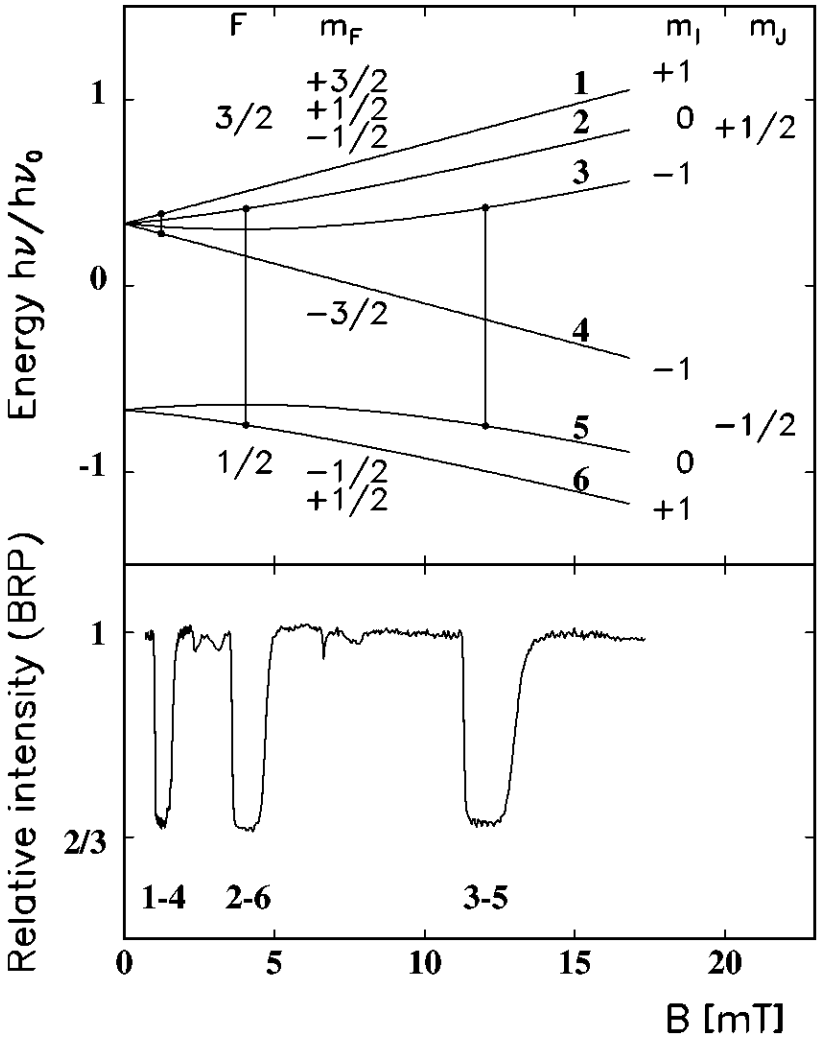

# Target polarimetry #2

Ion extraction polarimetry for direct measurement of $P_{zz}$

Done at NIKHEF and should have been done at MIT–Bates: exploits angular asymmetry of the $^3$H–$\overleftrightarrow{d}$ fusion process $^3\mathrm{H}(\mathrm{d},\mathrm{n})^4\mathrm{He}$

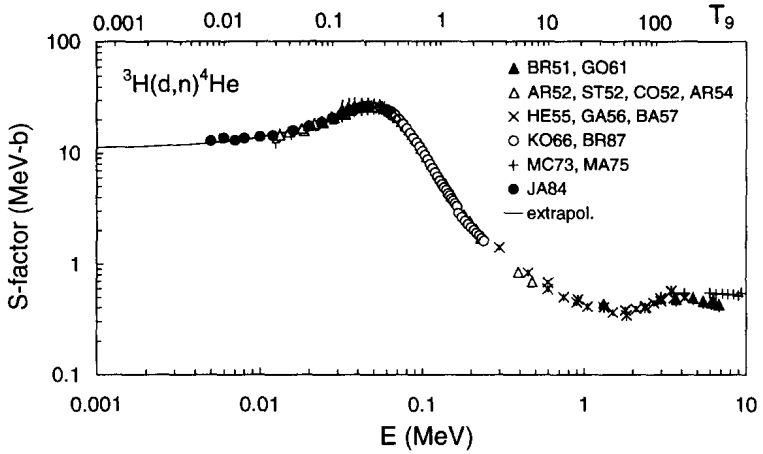


▷ $Q = +17.6\,\mathrm{MeV} \Longrightarrow T_n \approx 14.6\,\mathrm{MeV}$

▷ $60\,\mathrm{keV}$ deuterons $\Longrightarrow E = 36\,\mathrm{keV}$ in CM

▷ Huge cross-section, $\sigma(E) = (S(E)/E)\mathrm{e}^{-2\pi\eta} \approx 2.3\,\mathrm{b}$ (!)

Sommerfeld $\eta = 0.909$

▷ Key point: neutron asymmetry

$$n(\theta) \propto 1 - \frac{1}{4} f(E_d) P_{zz} (3\cos^2\theta - 1)$$

e.g. $f \approx 0.959$ at $E_d = 51\,\mathrm{keV}$ // Zhou++, NIMA **379**, 212 (1996)

# Target polarimetry #2



Ion extraction polarimetry for direct measurement of $P_{zz}$

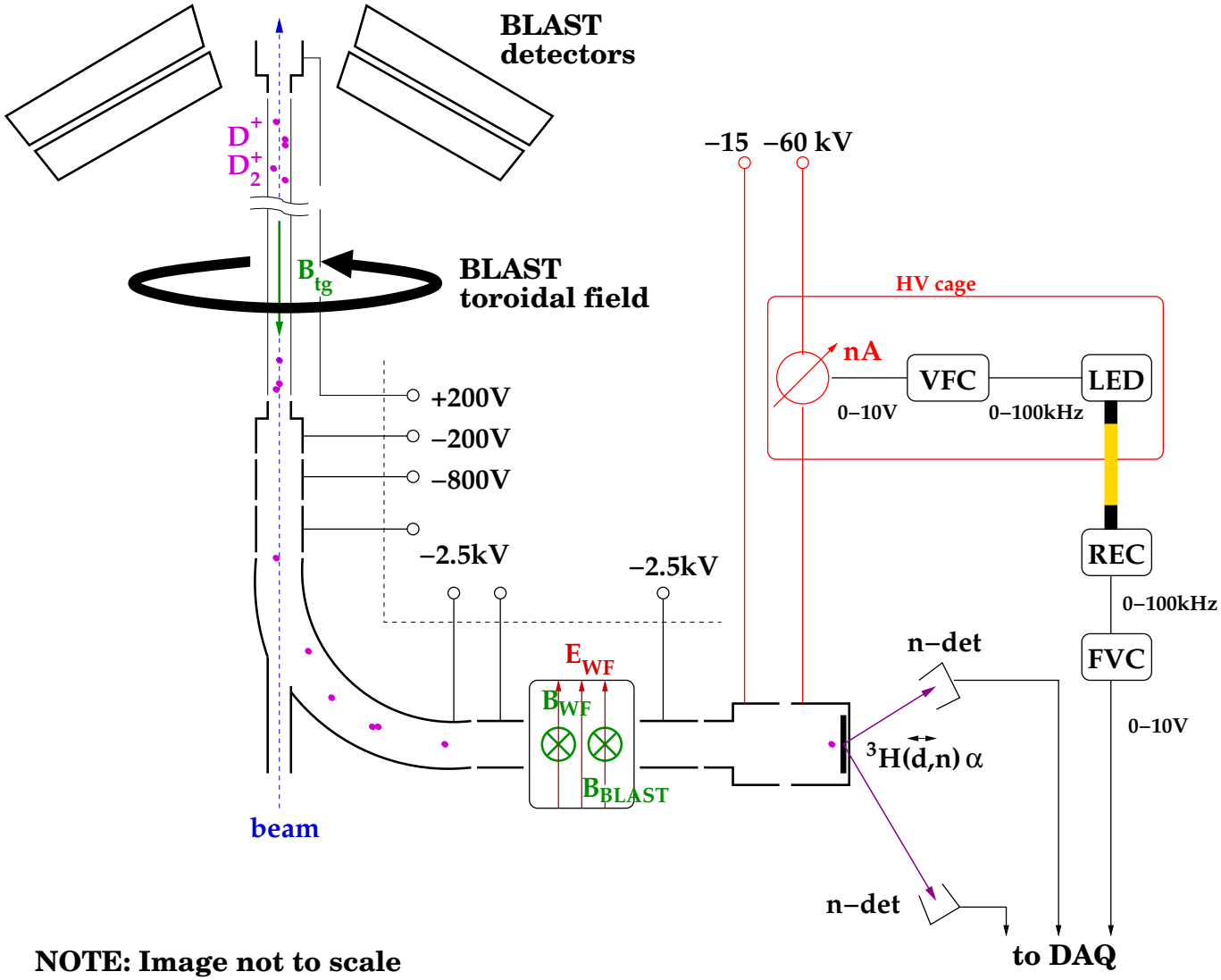


**NOTE: Image not to scale**

# Evidence of nuclear tensor polarization in deuterium molecules

$$P_{zz}^{\mathrm{tot}} = \frac{n_{\mathrm{D}} P_{zz}(\mathrm{D}) + 2n_{\mathrm{D}_2^{\mathrm{rec}}} P_{zz}(\mathrm{D}_2^{\mathrm{rec}})}{n_{\mathrm{D}} + 2n_{\mathrm{D}_2^{\mathrm{rec}}} + 2n_{\mathrm{D}_2^{\mathrm{unp}}}} = \xi\, P_{zz}(\mathrm{D}) + \zeta\, P_{zz}(\mathrm{D}_2^{\mathrm{rec}})$$

- Measured $P_{zz}(\mathrm{D})$ extracted from Teflon-coated Al cell vs. uncoated Cu cell by ion polarimetry: $P_{zz}^{+}(\mathrm{D}) = +0.523 \pm 0.005$ / $P_{zz}^{-}(\mathrm{D}) = -1.037 \pm 0.007$ vs. $P_{zz}^{+}(\mathrm{D}) = +0.434 \pm 0.027$ / $P_{zz}^{-}(\mathrm{D}) = -0.974 \pm 0.035$
- Determined $P_{zz}(\mathrm{D}_2)$ from asymmetry for electron–deuteron elastic scattering: $A_{\mathrm{ed}} = -0.232 \pm 0.014$ vs. $A_{\mathrm{ed}} = -0.183 \pm 0.043$

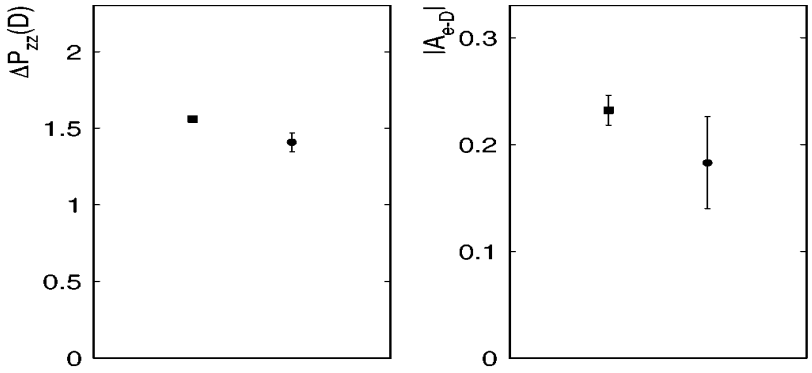


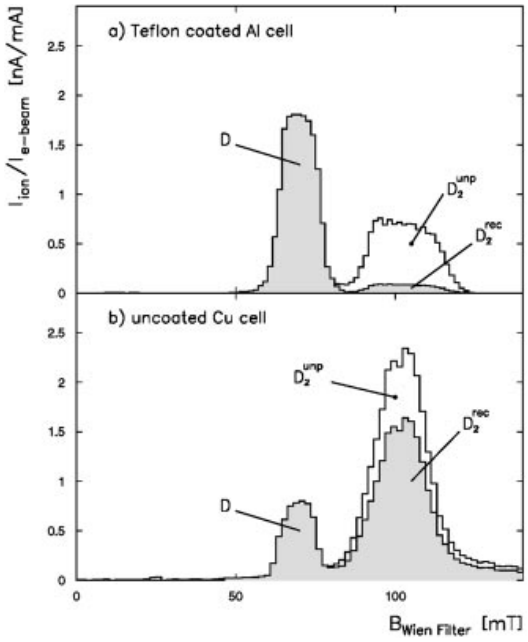


$\Longrightarrow \Delta P_{zz}(\mathrm{D}_2^{\mathrm{rec}}) = (0.81 \pm 0.32)\Delta P_{zz}(\mathrm{D})$

$\Longrightarrow$ May allow one to develop a robust polarized $\mathrm{H}_2/\mathrm{D}_2$ target insensitive to beam-induced depolarizations, polarization losses due to spin-exchange collisions, and radiation damage to cell surface

van den Brand++, PRL **78**, 1235 (1997)

# The ABC of e–d elastic scattering

- Spin(deuteron) = 1 $\Longrightarrow$ three form-factors $G_C(Q^2)$, $G_Q(Q^2)$ and $G_M(Q^2)$
- The unpolarized XS, $\sigma_0 = \sigma_{\text{Mott}} f_{\text{rec}}^{-1} S$, where $S = A(Q^2) + B(Q^2)\tan^2\theta_e/2$, allows for separation of two linear combinations of form-factors:

$$A(Q^2) = G_C^2 + \tfrac{8}{9}\eta^2 G_Q^2 + \tfrac{2}{3}\eta G_M^2\,, \quad B(Q^2) = \tfrac{4}{3}\eta(1+\eta)G_M^2\,, \quad \eta = Q^2/4M^2$$

$\Longrightarrow$ A polarized measurement is needed to disentangle $G_C$ from $G_Q$

$$\sigma = \sigma_0\left[1 + \frac{P_{zz}A_d^T}{\sqrt{2}}\right], \quad A_d^T = \sum_{i=0}^{2} d_{2i}T_{2i}$$

$$d_{20} = \frac{3\cos^2\theta^* - 1}{2}, \quad d_{21} = -\sqrt{\frac{3}{2}}\sin 2\theta^*\cos\phi^*, \quad d_{22} = \sqrt{\frac{3}{2}}\sin^2\theta^*\cos 2\phi^*$$

- Tensor analyzing powers (access controlled by spin angles $(\theta^*, \phi^*)$):

$$T_{20} = -\frac{1}{\sqrt{2}S}\left[\frac{8}{3}\eta\, G_C G_Q + \frac{8}{9}\eta^2 G_Q^2 + \frac{1}{3}\eta\left(1 + 2(1+\eta)\tan^2\frac{\theta_e}{2}\right)G_M^2\right]$$

$$T_{21} = -\frac{2}{\sqrt{3}S}\sqrt{\eta^3\left(1 + \eta\sin^2\frac{\theta_e}{2}\right)}\, G_Q G_M \sec\frac{\theta_e}{2}$$

$$T_{22} = -\frac{2}{2\sqrt{3}S}\eta G_M^2$$

# Deuteron elastic structure functions

(not state-of-the-art)

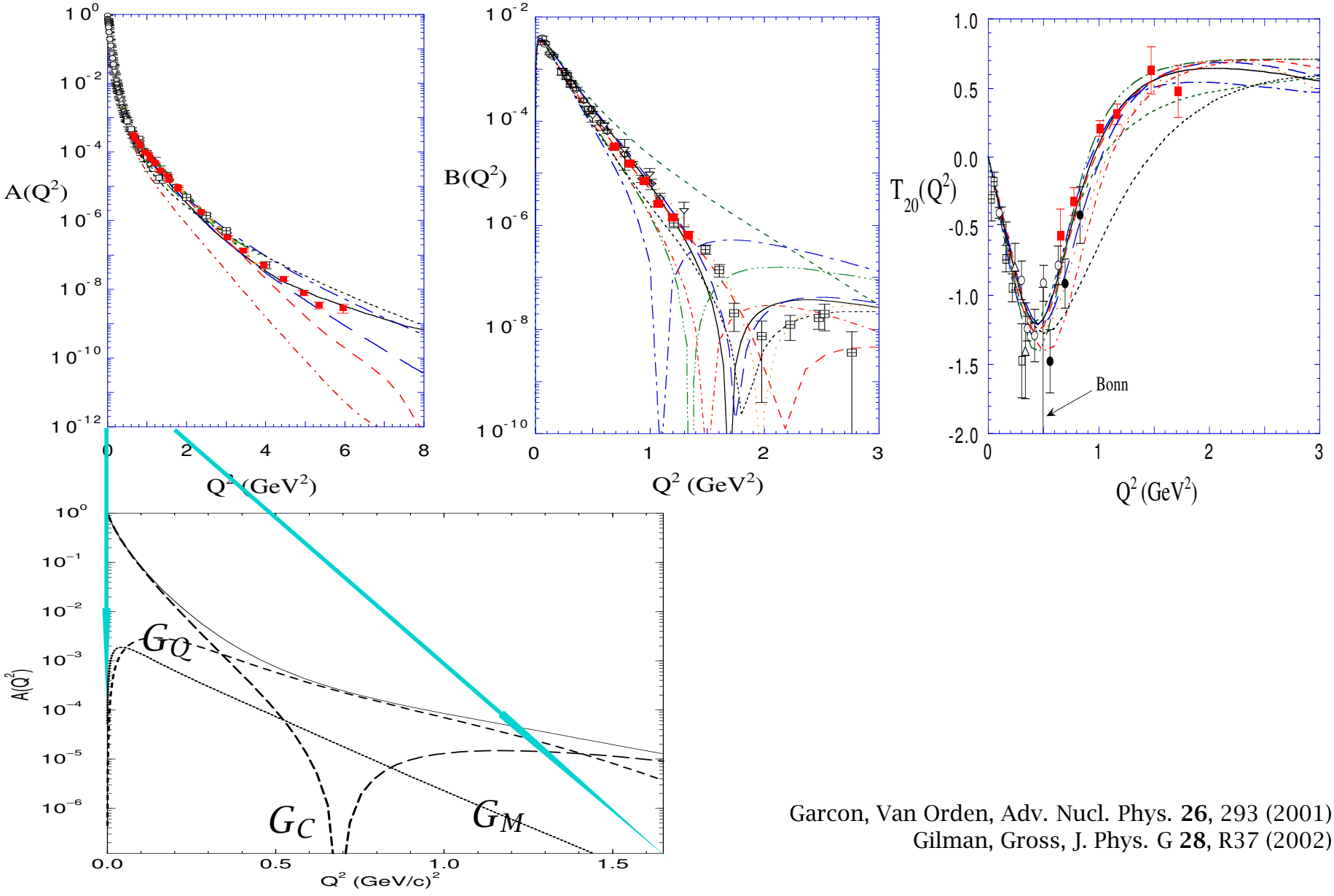


Garcon, Van Orden, Adv. Nucl. Phys. **26**, 293 (2001)
Gilman, Gross, J. Phys. G **28**, R37 (2002)

# The $T_{20}(70°)$ results from NIKHEF

1996: a single point in $T_{20}$ and $T_{22}$, small contribution from $T_{21}$ estimated from existing data on $G_Q(Q^2)$ and $B(Q^2)$

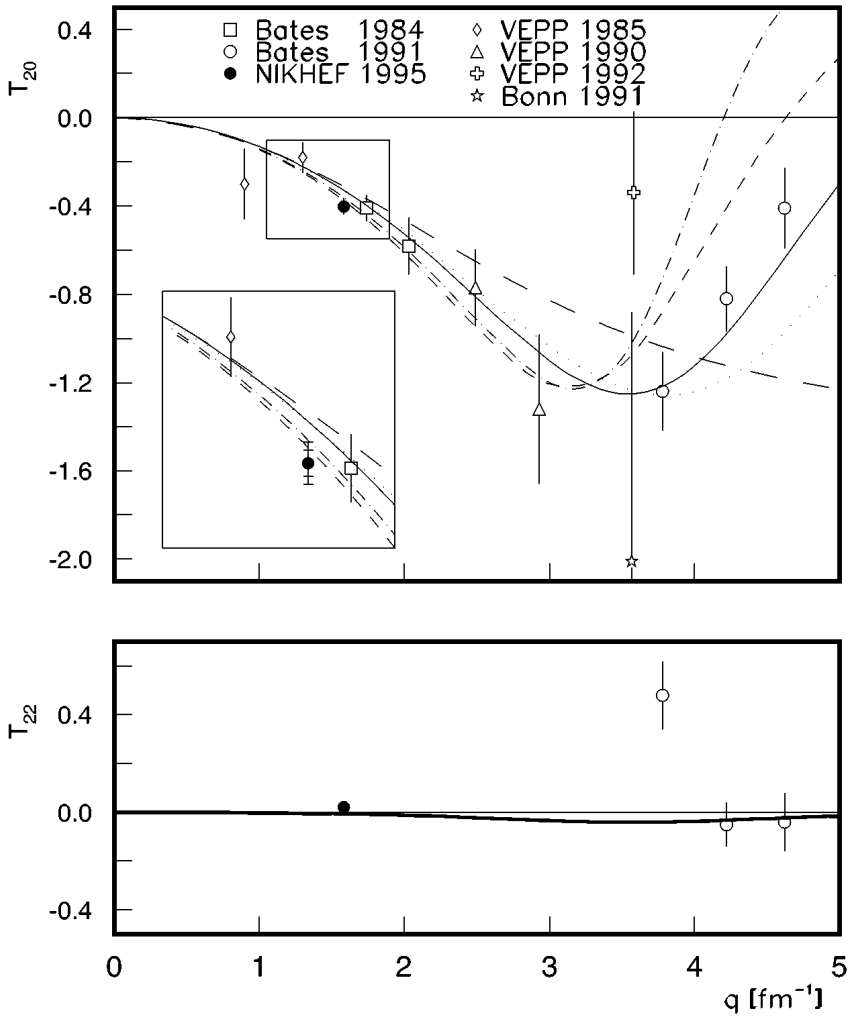


Ferro-Luzzi++, PRL **77**, 2630 (1996)

1999: three new points, with absolute polarimetry

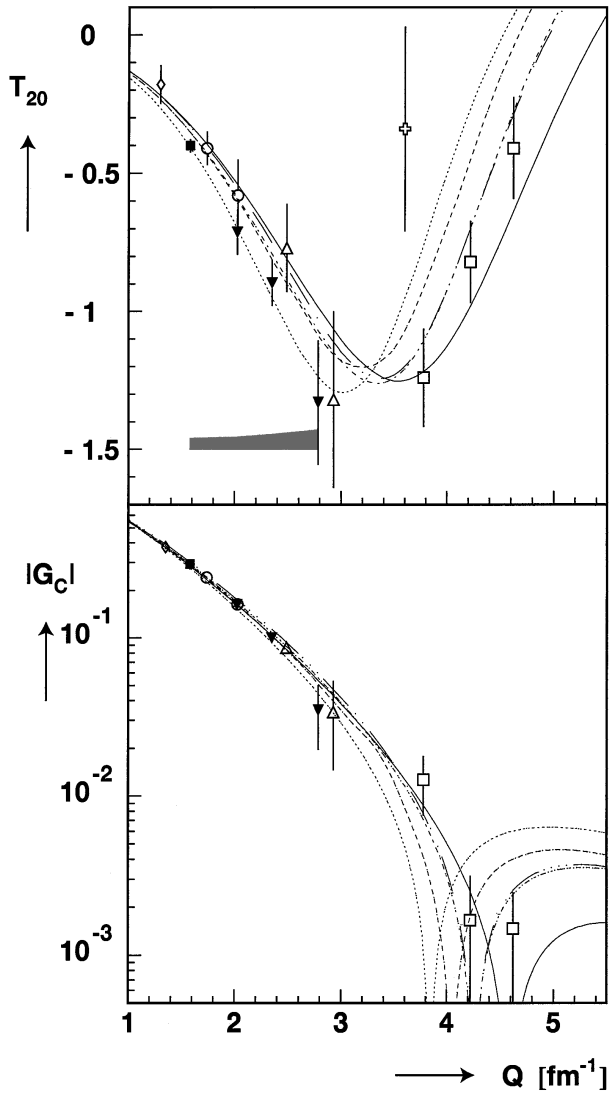


Bouwhuis++, PRL **82**, 3755 (1999)

# The $T_{20}(70°)$ results from MIT–Bates

- The 1984 and 1991/1994 MIT–Bates experiments yielded deuteron tensor polarizations $t_{20}$ via $\mathrm{d}(\mathrm{e},\mathrm{e}'\overleftrightarrow{\mathrm{d}})$ by using recoil polarimetry

  Schulze++, PRL **52**, 597 (1984)
  The++, PRL **67**, 173 (1991)
  Garçon++, PRC **49**, 2516 (1994)

- The 2004/2005 experiments at BLAST (using ABS) extracted $T_{20}$ and $T_{21}$ like at NIKHEF
  - ▷ Small $T_{22}$ contribution subtracted by using a parameterization of previous low-$Q$ data
  - ▷ In absence of absolute polarimetry, polarization and spin angle calibrated by the two lowest-$Q$ points

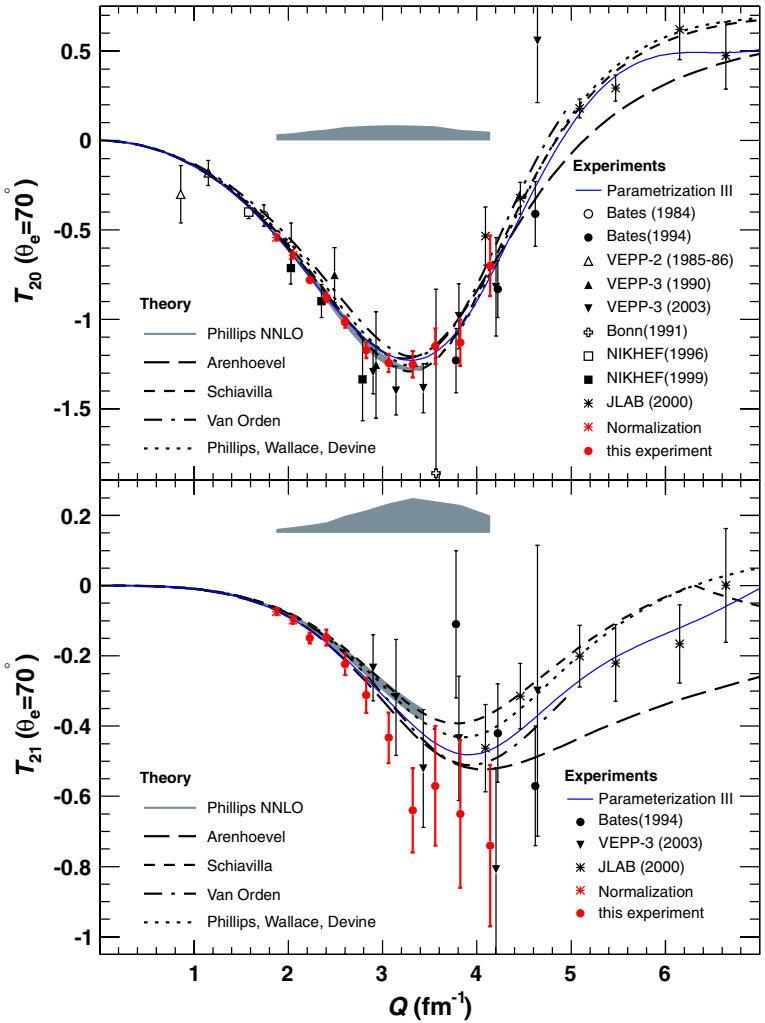


Zhang++, PRL **107**, 252501 (2011)

# $\tilde{T}_{20R}$ from BLAST

Eliminate the dependence on $\theta_e$ and $G_M$; in addition, divide out the leading $Q^2$-dependence ("reduced $T_{20}$"):

$$\tilde{T}_{20} = -\frac{\frac{8}{3}\eta G_C G_Q + \frac{8}{9}\eta^2 G_Q^2}{\sqrt{2}\left(G_C^2 + \frac{8}{9}\eta^2 G_Q^2\right)}, \quad \tilde{T}_{20R}(Q^2) = -\frac{3}{\sqrt{2}Q_d Q^2}\tilde{T}_{20}(Q^2)$$

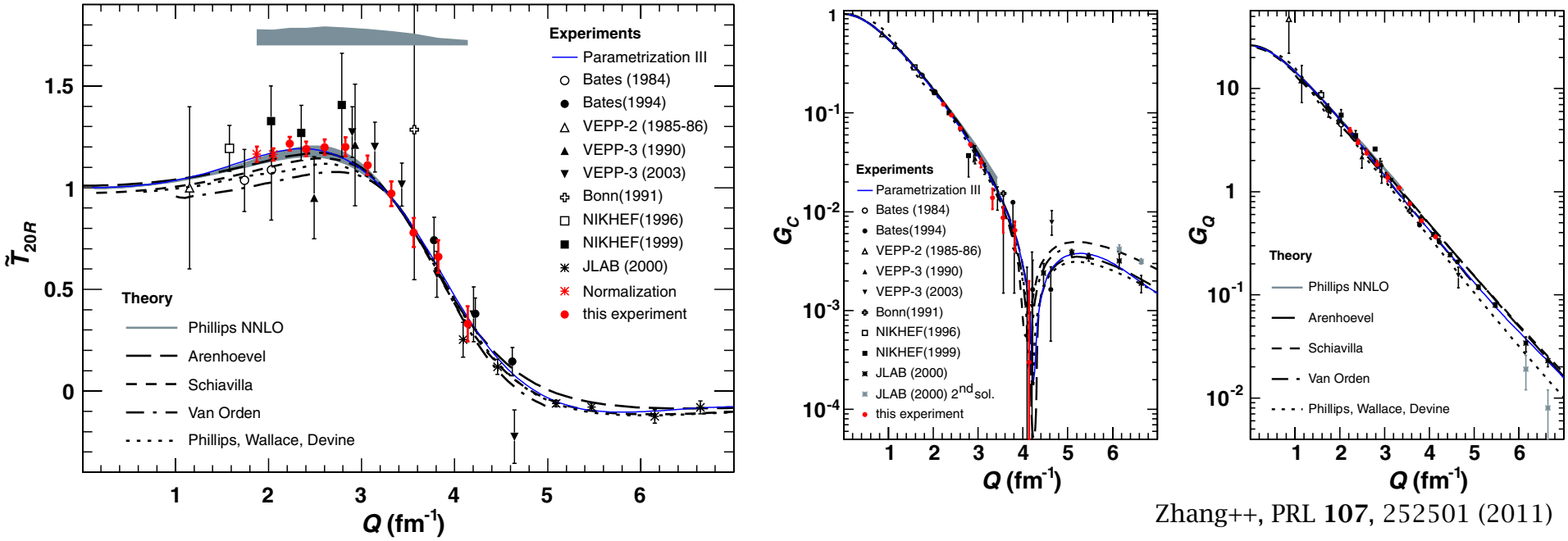


Zhang++, PRL **107**, 252501 (2011)

- Precise data covering the minimum of $T_{20}$ and the first node of $G_C$
- Strong constraint on models

# $T_{11}^{e}$ from BLAST (e–d elastic)

With polarized beam and vector-polarized target, $A_{ed}^{V}$ becomes accessible:

$$\sigma = \sigma_0 \left[ 1 + \sqrt{\frac{1}{2}} P_{zz} A_d^T + \sqrt{\frac{3}{2}} P_e P_z A_{ed}^V \right]$$

$$A_{ed}^{V} = \sqrt{3} \left( \frac{1}{\sqrt{2}} \cos\theta^* T_{10}^{e}(Q^2, \theta_e) - \sin\theta^* \cos\phi^* T_{11}^{e}(Q^2, \theta_e) \right)$$

$$T_{11}^{e} \propto G_M \left( G_C + \frac{\eta}{3} G_Q \right) \text{ – measured for the first time :}$$

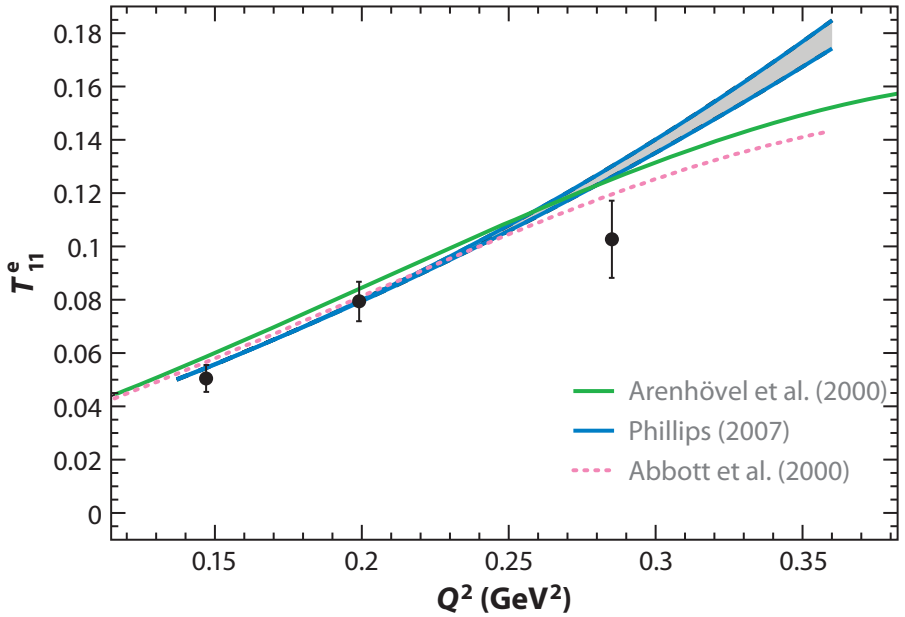


Hasell++, Annu. Rev. Nucl. Part. Sci. **61**, 409 (2011)

# The ABC of e–d quasi-elastic scattering #1

$$\frac{d^5\sigma}{d\omega d\Omega_e d\Omega_p} = k\sigma_{ep}\rho(p_r)$$

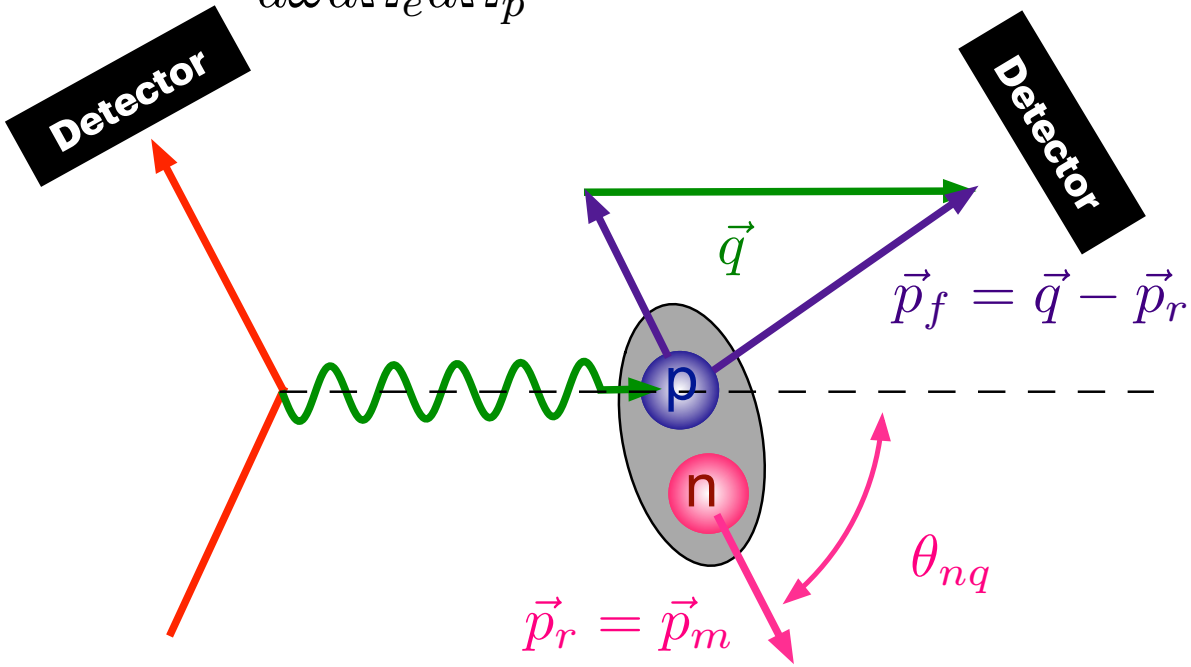


In the plane wave impulse approximation (PWIA)

$$\rho(p_r) = \frac{\sigma_{exp}}{k\sigma_{ep}}$$

N. Santiesteban (Trento 2023)

# The ABC of e–d quasi-elastic scattering #2

PWIA

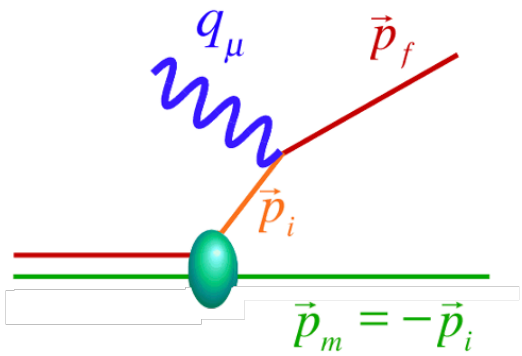


FSI

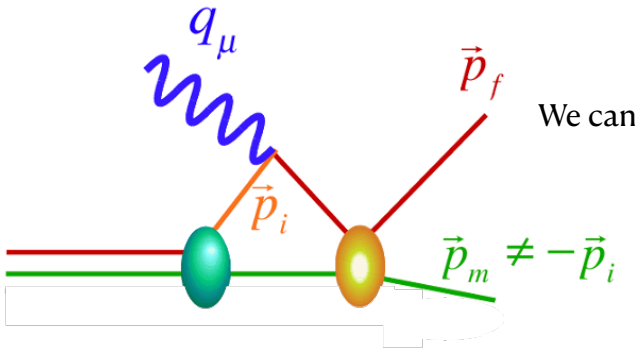


We can reduce at the right kinematics

**In reality ...**

MEC

$Q^2 > 2GeV^2$

Suppresses MEC

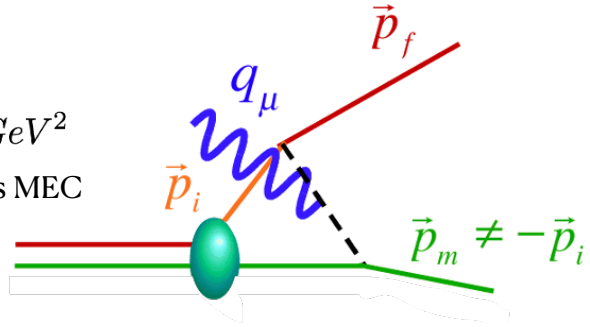


IC

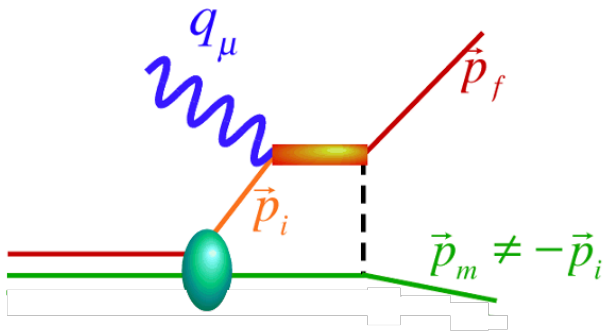


$x > 1$

Suppresses IC

N. Santiesteban (Trento 2023)

# $A_{ed}^{V}(\theta^* = 90°, \phi^* = 0°)$ in quasi-elastic $^2\vec{H}(\vec{e}, e'n)$ — NIKHEF

$$\sigma = \sigma_0 \left[ 1 + P_1^d A_d^V + P_2^d A_d^T + hP_e \left( A_e + P_1^d A_{ed}^V + P_2^d A_{ed}^T \right) \right]$$

$$P_1^d = \sqrt{\frac{3}{2}}(n_+ - n_-)$$

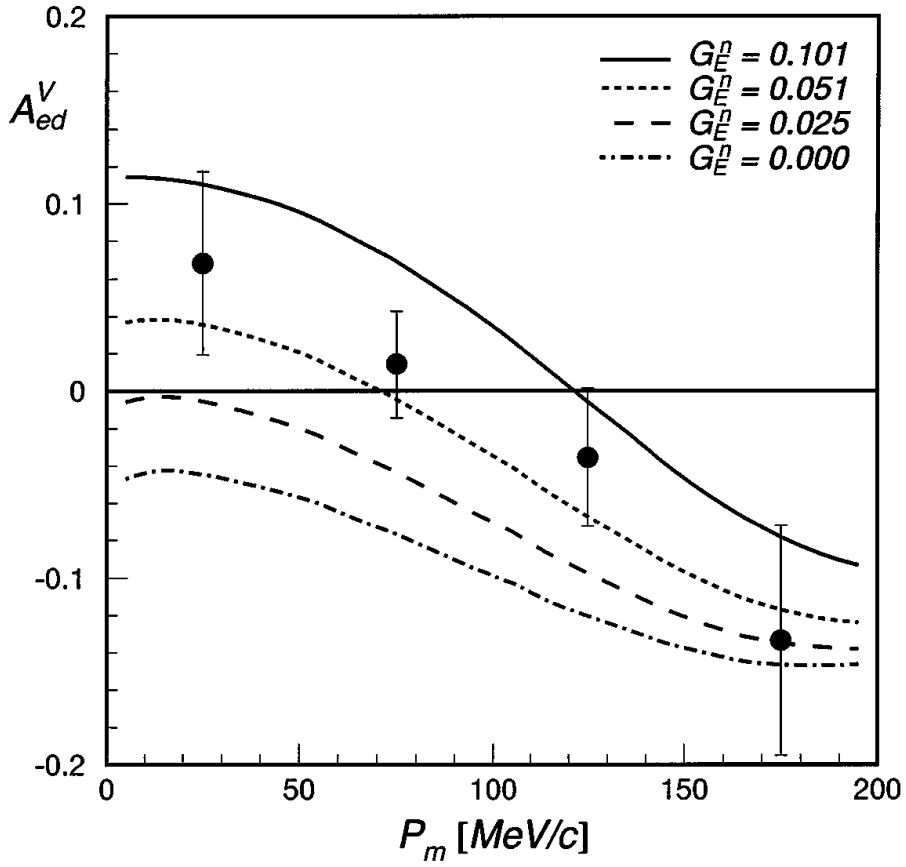


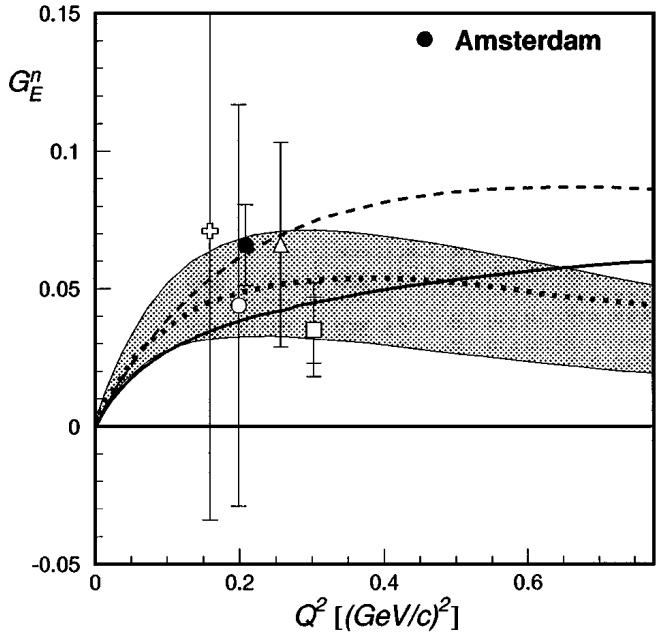


$$A_{ed}^V \approx a \cos\theta^* + b \frac{G_E^n}{G_M^n} \sin\theta^* \cos\phi^*$$

... from the days when each $Q^2$-point was precious ... Passchier++, PRL **82**, 4988 (1999)

# $A_{ed}^{V}(\theta^* = 90°, \phi^* = 0°)$ in quasi-elastic $^2\vec{H}(\vec{e}, e'p)$ — NIKHEF

**Very nice:** $p_{miss}$ dependence of $A_{ed}^{V}(\theta^* = 90°, \phi^* = 0°)$ at $Q^2 = 0.21$ (GeV/$c$)$^2$:

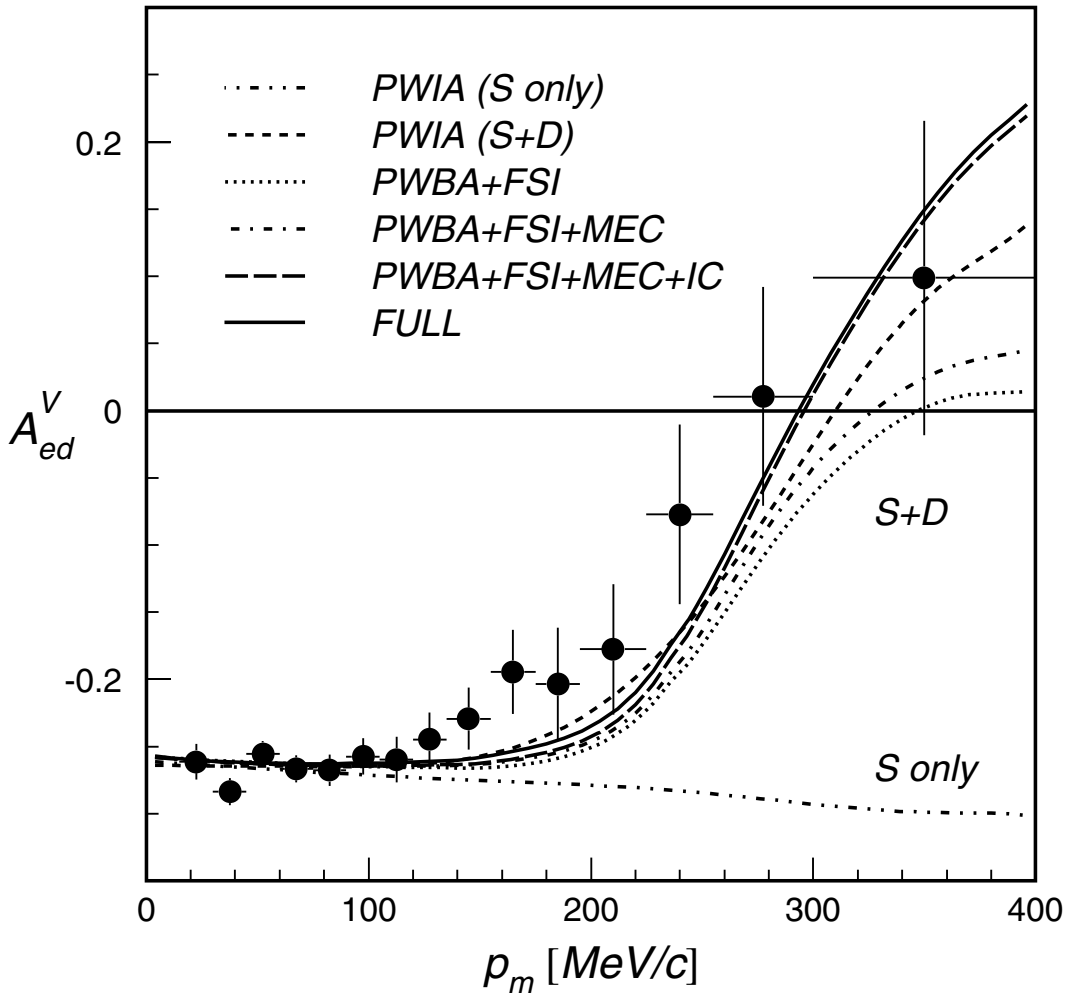


Passchier++, PRL **88**, 102303 (2002)

# Sidetrack: $^3\vec{\mathrm{He}}(\vec{e},e'd)$ & $^3\vec{\mathrm{He}}(\vec{e},e'p)$ KRAKOW/BOCHUM CALC.

Motivation behind the 2009 BigFamily of polarized-$^3$He experiments in Hall A — incidentally, using BigBite (!)

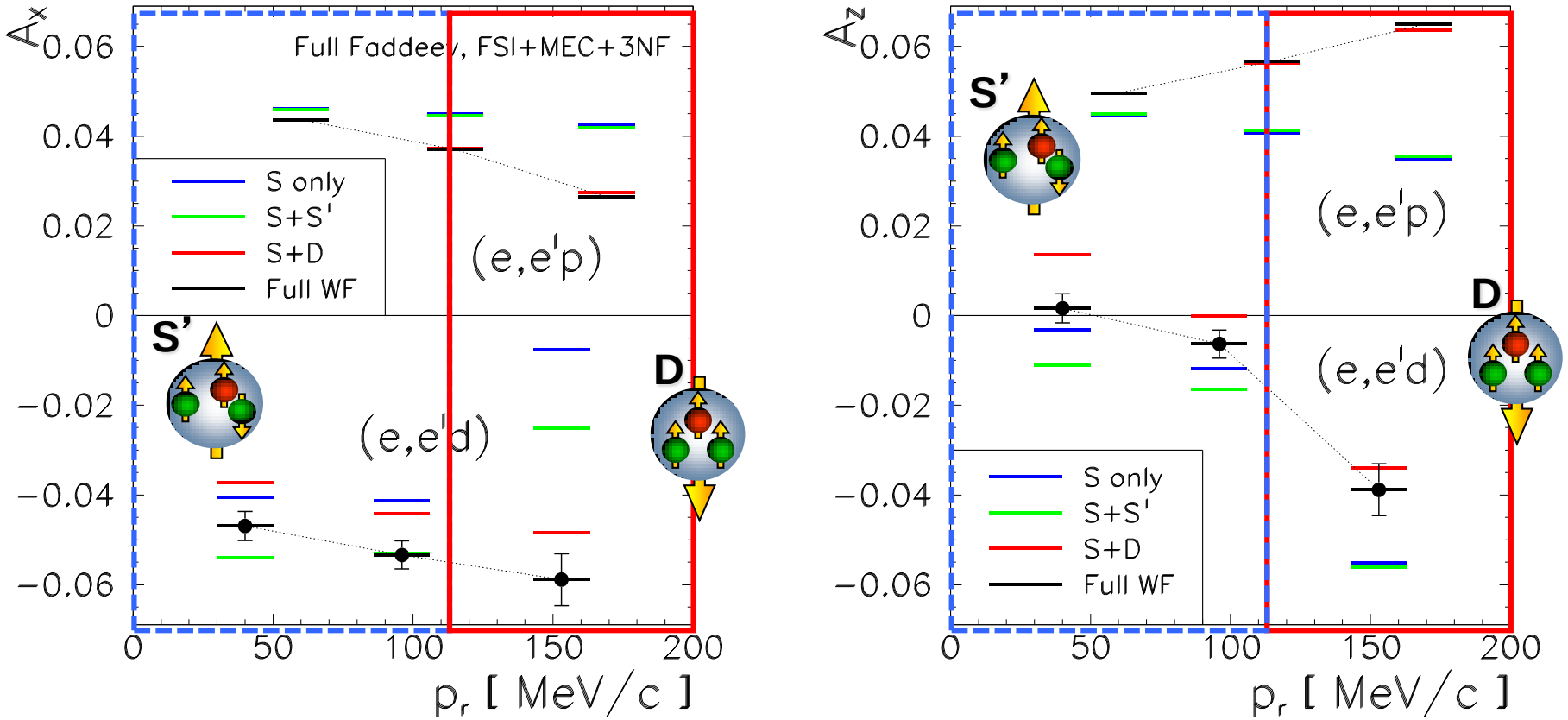


- $S'$ state relevant at small $p_r$ (= $p_{\mathrm{miss}}$)?
- $D$ state governs variation of $A_z$ at large $p_r$?

For answers, see Mihovilovič++, PRL **113**, 232505 (2014) and PLB **788**, 117 (2019)

# ... but the true ground state of $^3$He is like lace

| Channel number | $L$ | $S$ | $l_\alpha$ | $L_\alpha$ | $P$ | $K$ | Probability (%) |
|---|---|---|---|---|---|---|---|
| 1 | 0 | 0.5 | 0 | 0 | $A$ | 1 | 87.44 |
| 2 | 0 | 0.5 | 0 | 0 | $M$ | 2 | 0.74 |
| 3 | 0 | 0.5 | 1 | 1 | $M$ | 1 | 0.74 |
| 4 | 0 | 0.5 | 2 | 2 | $A$ | 1 | 1.20 |
| 5 | 0 | 0.5 | 2 | 2 | $M$ | 2 | 0.06 |
| 6 | 1 | 0.5 | 1 | 1 | $M$ | 1 | 0.01 |
| 7 | 1 | 0.5 | 2 | 2 | $A$ | 1 | 0.01 |
| 8 | 1 | 0.5 | 2 | 2 | $M$ | 2 | 0.01 |
| 9 | 1 | 1.5 | 1 | 1 | $M$ | 1 | 0.01 |
| 10 | 1 | 1.5 | 2 | 2 | $M$ | 2 | 0.01 |
| 11 | 2 | 1.5 | 0 | 2 | $M$ | 2 | 1.08 |
| 12 | 2 | 1.5 | 1 | 1 | $M$ | 1 | 2.63 |
| 13 | 2 | 1.5 | 1 | 3 | $M$ | 1 | 1.05 |
| 14 | 2 | 1.5 | 2 | 0 | $M$ | 2 | 3.06 |
| 15 | 2 | 1.5 | 2 | 2 | $M$ | 2 | 0.18 |
| 16 | 2 | 1.5 | 3 | 1 | $M$ | 1 | 0.37 |

Blankleider, Woloshyn PRC **29**, 538 (1984)

# $A_d^T$ in quasi-elastic $^2\vec{\vec{H}}(e, e'p)$ — NIKHEF

Probes spin-dependent momentum densities $\rho_{m_z}$:

$$\rho_0(\boldsymbol{p}) \propto \left[R_0 + \sqrt{2}R_2 d^2_{0,0}(\theta)\right]^2 + 3\left[R_2 d^2_{1,0}(\theta)\right]^2$$

$$\rho_{\pm1}(\boldsymbol{p}) \propto \left[R_0 - \tfrac{1}{\sqrt{2}}R_2 d^2_{0,0}(\theta)\right]^2 + \tfrac{9}{8}R_2^2(1-\cos^4\theta)$$

$$A_d^T = \sqrt{\frac{1}{2}}\frac{\sigma_+(p_m) + \sigma_-(p_m) - 2\sigma_0(p_m)}{\sigma_+(p_m) + \sigma_-(p_m) + \sigma_0(p_m)} \overset{\text{PWIA}}{=} -\frac{2R_0(p)R_2(p) + \sqrt{\frac{1}{2}}R_2^2(p)}{R_0^2(p) + R_2^2(p)} d^2_{0,0}(\theta)$$

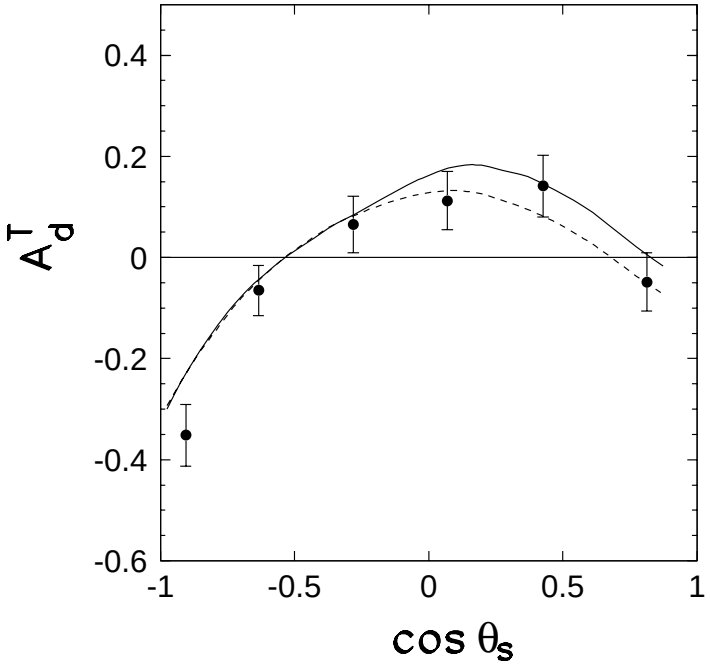


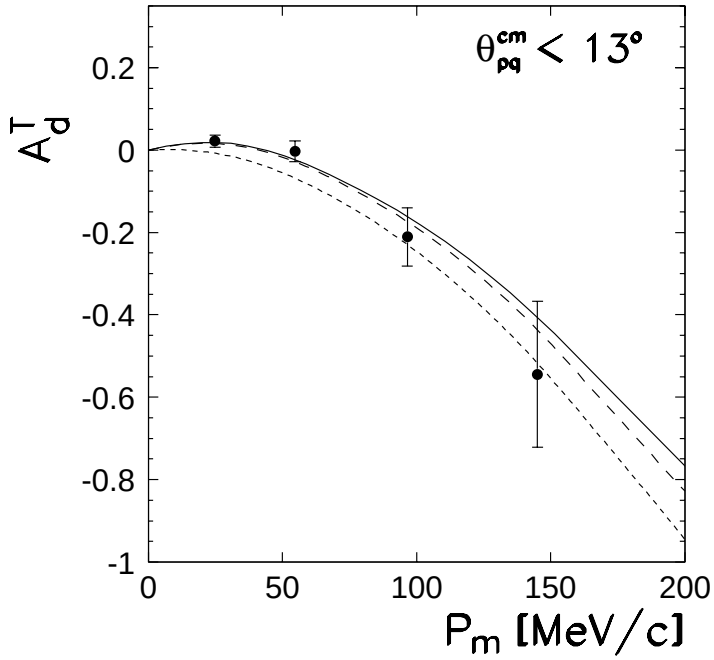


- One of the many statements that FSI, MEC & RC are needed

Zhou++, PRL **82**, 687 (1999)

# $A_{ed}^{V}$ / $A_{d}^{T}$ in QE $^2\vec{H}(\vec{e}, e'n)$ / $^2\overleftrightarrow{H}(e, e'n)$ — BLAST

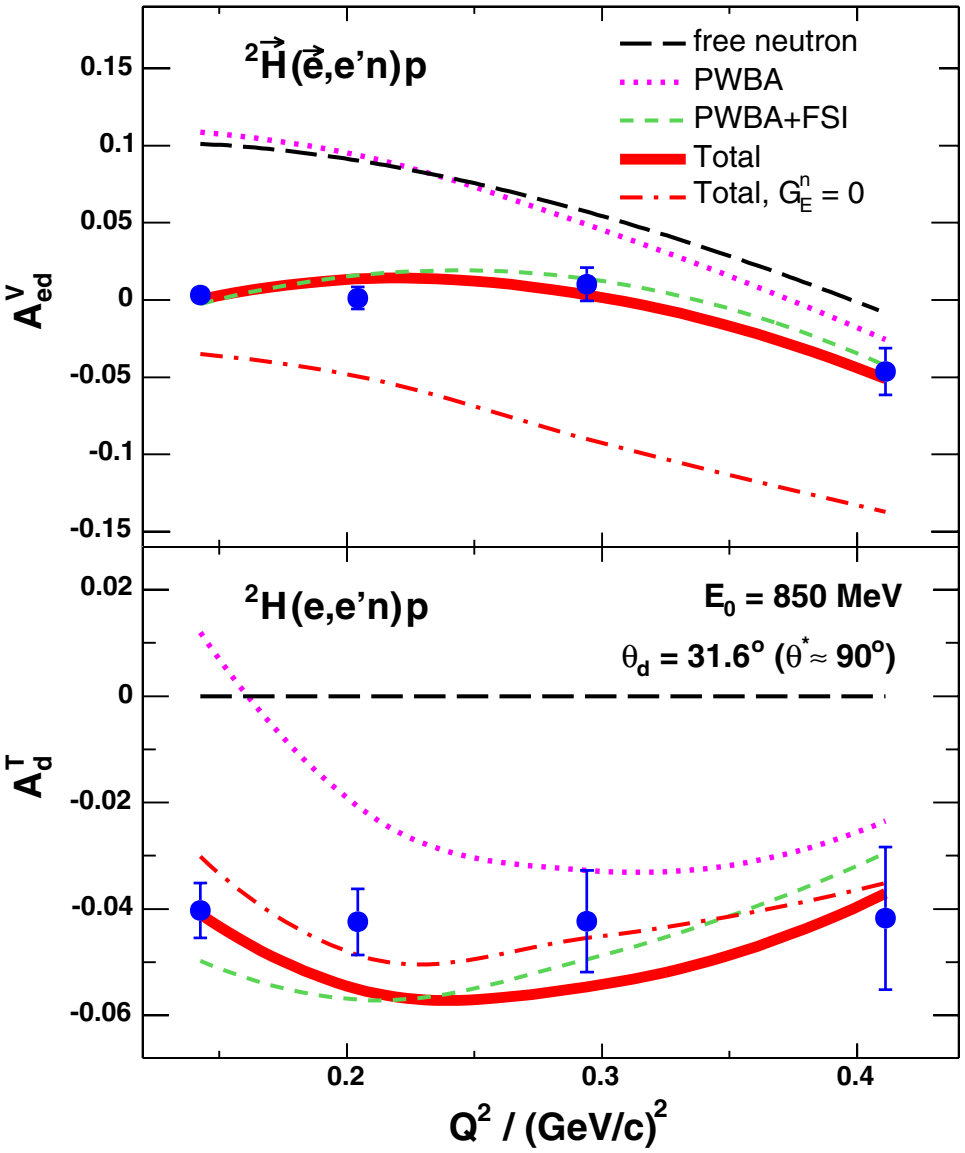


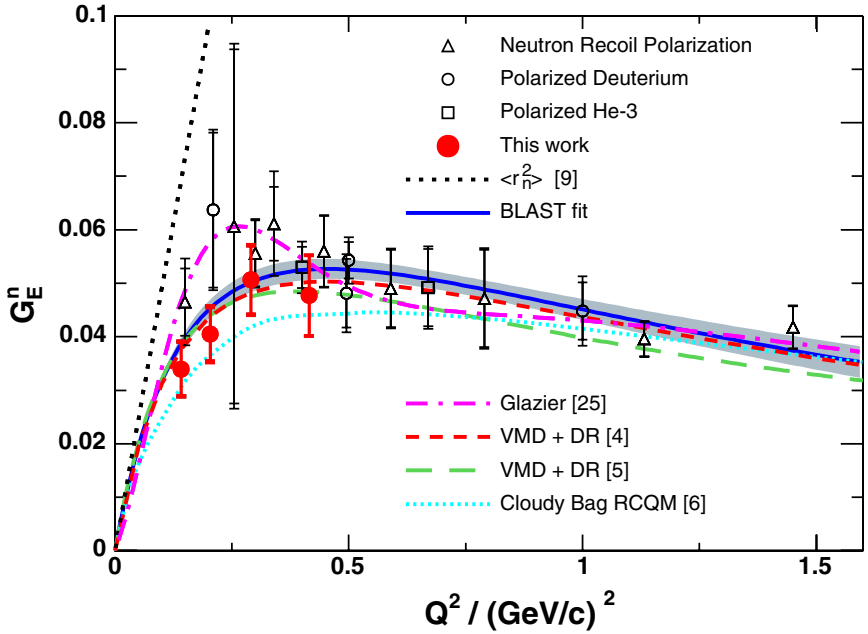


Geis++, PRL **101**, 042501 (2008)

# $A_{ed}^{V}$ / $A_{d}^{T}$ in QE $^{2}\vec{H}(\vec{e}, e'p)$ / $^{2}\overleftrightarrow{H}(e, e'p)$ — BLAST

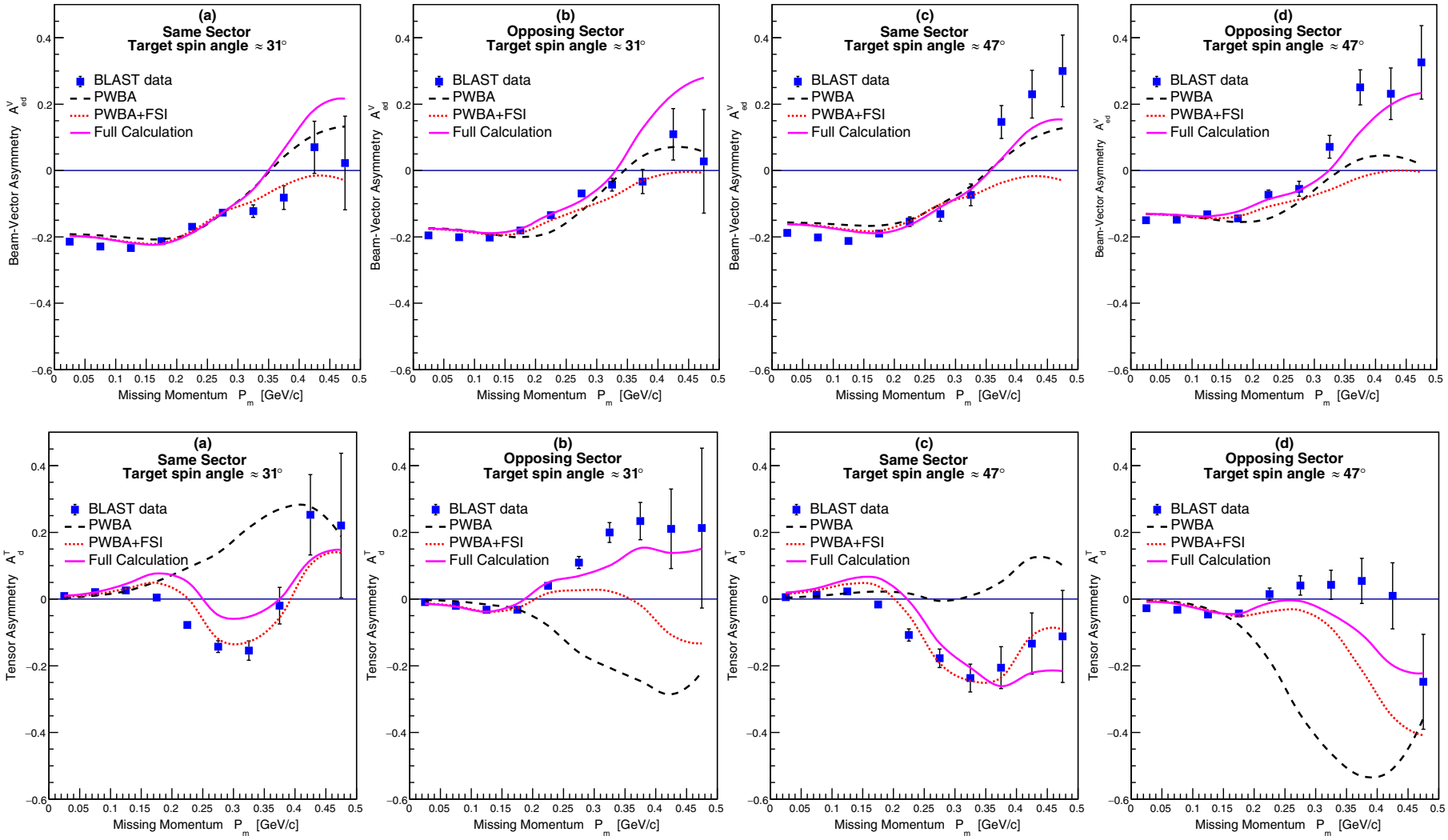


DeGrush++, PRL **119**, 182501 (2017)

# Conclusions

- *O wondrous ABS!*
- Groundbreaking vector/tensor deuteron work at NIKHEF ...
- ... which was inherited by & bore more fruit at MIT–Bates
- BLAST: lots of stuff on tape & not analyzed
- Good polarimetry is essential